Space Sci Rev (2009) 147: 187–231
DOI 10.1007/s11214-009-9496-7

Dynamics of the Earth's Particle Radiation Environment

Rami Vainio · Laurent Desorgher · Daniel Heynderickx · Marisa Storini · Erwin Flückiger · Richard B. Horne · Gennady A. Kovaltsov · Karel Kudela · Monica Laurenza · Susan McKenna-Lawlor · Hanna Rothkaehl · Ilya G. Usoskin

Received: 12 November 2008 / Accepted: 19 February 2009 / Published online: 11 March 2009

Abstract The physical processes affecting the dynamics of the Earth's particle radiation environment are reviewed along with scientific and engineering models developed for its description. The emphasis is on models that are either operational engineering models or

R. Vainio (✉)
Department of Physics, University of Helsinki, Helsinki 00014, P.O.B. 64, Finland
e-mail: rami.vainio@helsinki.fi

L. Desorgher
SpaceIT GmbH, Sennweg 15, 3012 Bern, Switzerland

D. Heynderickx
DH Consultancy, Diestsestraat 133/3, 3000 Leuven, Belgium

E. Flückiger
University of Bern, Bern, Switzerland

R.B. Horne
British Antarctic Survey, Cambridge, UK

G.A. Kovaltsov
Ioffe Physical-Technical Institute, 194021 St. Petersburg, Russia

K. Kudela
Slovak Academy of Sciences, Kosice, Slovakia

M. Laurenza · M. Storini
IFSI-Roma/INAF, Via del Fosso del Cavaliere, 100, 00133 Roma, Italy

S. McKenna-Lawlor
Space Technology Ireland, National University of Ireland, Maynooth, Co. Kildare, Ireland

H. Rothkaehl
Polish Academy of Sciences, Warsaw, Poland

I.G. Usoskin
Sodankylä Geophysical Observatory (Oulu unit), University of Oulu, Oulu 90014, Finland

models presently under development for this purpose. Three components of the radiation environment, i.e., galactic cosmic rays (GCRs), solar energetic particles (SEPs) and trapped radiation, are considered separately. In the case of SEP models, we make a distinction between statistical flux/fluence models and those aimed at forecasting events. Models of the effects of particle radiation on the atmosphere are also reviewed. Further, we summarize the main features of the models and discuss the main outstanding issues concerning the models and their possible use in operational space weather forecasting. We emphasize the need for continuing the development of physics-based models of the Earth's particle radiation environment, and their validation with observational data, until the models are ready to be used for nowcasting and/or forecasting the dynamics of the environment.

Keywords Radiation environment · Solar energetic particles · Radiation belts · Cosmic rays · Radiation effects

1 Introduction

The Earth's particle radiation environment consists of several components of ionizing radiation: (i) galactic cosmic rays (GCRs); (ii) solar energetic particles (SEPs); and (iii) radiation-belt particles. Each of these particle populations has its own characteristics with respect to origin, particle abundances, spatial and energy distributions, and temporal variations.

According to the current paradigm, GCRs are produced by diffusive shock acceleration in supernova remnants (e.g., Blandford and Eichler 1987) from which they diffuse to fill the whole galaxy. In order to be observed at Earth, these charged particles have to penetrate the electromagnetic fields of the heliosphere, i.e., the region of space around the Sun (extending to further than 100 AU) dominated by the solar-wind plasma and by the interplanetary magnetic field (IMF). Thus, the GCR flux in near-Earth space is controlled by solar magnetic activity and follows an 11-year cycle that is in anticorrelation with the main solar activity indices (e.g., the sunspot number). In addition, the GCR flux responds to solar-wind variations on both long and short time scales. SEPs, on the other hand, comprise events that are well correlated with coronal mass ejections (CMEs) and solar flares (e.g., Reames 1999). Thus, the occurrence of SEPs is in positive correlation with ongoing solar activity.

The radiation belts consist of particles trapped by the Earth's magnetic field, mainly electrons and protons, accelerated locally by magnetospheric processes, or produced through trapping of SEPs during geomagnetic activity or through the cosmic-ray albedo neutron decay (CRAND) process (Singer 1958), in which a fraction of the neutrons produced by high-energy cosmic rays (CRs) undergoing nuclear interactions in the Earth's atmosphere decays into protons and electrons inside the geomagnetic field.

Overall, the radiation environment of the Earth is very dynamic. Even the most stable component of the radiation (i.e., the GCRs) varies by an order of magnitude at energies below a few hundred MeV per nucleon due to heliospheric modulation. SEP events can produce increases of several orders of magnitude in the fluxes of energetic ions (above 1 MeV per nucleon) and electrons (above 100 keV), which can last from a few hours to a week. Also the electron flux variations in the outer radiation belt can vary by over five orders of magnitude on time scales ranging from a few minutes to a few days (Baker and Kanekal 2008). Satellite malfunctions (and in some cases even the loss of spacecraft) have been linked to these variations and they also pose a hazard to astronauts in space (see Sect. 2). It is, thus, extremely important to understand the physical processes responsible for these variations so that better models can be developed to specify the state of SEP events and

radiation belt dynamics at those periods of high risk affecting satellite operators, designers, and insurers.

The purpose of this paper is to review the physical processes affecting the variability of the terrestrial radiation environment, to review scientific models addressing these variations, and to present engineering models of the environment from the point of view of their capability to address variability occurring on different time scales. Finally, we list some of the major scientific challenges and outstanding issues concerning these engineering models.

2 Motivation: Radiation Effects

2.1 Effects on Electronics

Spacecraft can display anomalous behavior and failure following electric discharge events caused by plasma induced charging incurred in space. In addition, both spacecraft subsystems and scientific instrumentation in the payload can malfunction due to impinging electromagnetic and particle radiation (McKenna-Lawlor 2008).

Electric discharges (due to plasma-induced surface charging and energetic-electron-induced internal charging) can affect communications with, and the control and operations of, particular spacecraft. Spacecraft charging depends both on the pertaining spacecraft geometry and on the orbit traversed since the characteristics of the natural environment differ across the range from low Earth orbit (LEO, at ~100–1000 km altitude) to beyond geosynchronous orbit (GEO, at ~36 000 km).

Discharge related electrical transients can appear to a spacecraft system as directions from the ground (phantom commands). In addition, thruster firings can produce changes in the ambient plasma environment that trigger arc discharges. Such unpredicted events may result in loss of control of the power and propulsion systems of a spacecraft and of individual on-board scientific instruments. Induced mode switching in which a spacecraft or an on-board instrument puts itself into Standby Mode, or otherwise changes its expected operational procedure, can also take place.

An important contribution to radiation effects is provided by charging inside dielectric materials and on ungrounded metallic parts of a spacecraft. High energy electrons from the radiation belts give rise to this charging and ensuing electric discharges can generate deleterious, on-board, electromagnetic interference.

Several methods have been proposed to combat surface and internal charging including: passive methods (using sharp spikes and high secondary emission coefficient surface materials) as well as active methods (using controlled emissions of electrons, ions, plasmas, neutral gas, and polar molecules). Mitigation of deep dielectric charging is under development (Lai 2003).

When a single particle causes a malfunction in common on-board electronic components the response produced is called a single event effect (SEE). These events occur when the ionization track in a sensitive region of a component produces a status flip, a signal transient or the following of destructive current paths (Holmes Siedle and Adams 2002; Hilgers et al. 2007). Charge deposition can, in addition, arise from the products of nuclear spallation reactions between protons or neutrons and nuclei of the materials making up the component. In consequence, trapped proton radiation, SEP events and GCRs, each with their inherent variations, can provide significant contributions to such effects. Radiation background in sensors constitutes a particular class of SEE.

Energetic particles can also pass through the protective coverings of the solar cells on a spacecraft, producing both ionization damage and displacement damage (crystal lattice

defects). Ongoing degradation in solar cell performance, made manifest by a reduction in their voltage and current outputs, occurs in consequence.

2.2 Biological Effects

Biological effects due to radiation, which pose a major risk to manned space flight, are also of concern to aircrews. When an organism is irradiated, part of the energy of the radiation is deposited into cells, which can be damaged or even die. This can lead to severe health problems. Radiation effects on humans are divided in two categories. Deterministic effects are produced when a person is exposed to a large dose of radiation for a limited time and these range from hair loss or nausea to acute sickness, or death. Stochastic effects are due to random radiation-induced changes at the DNA level leading, for example, to cancer. For a future manned mission to Mars or to the Moon it is presently a major problem to assess and limit the risk of stochastic effects due to long term exposure to GCRs as well as the risk of deterministic effects due to short term exposure to SEPs. With regard to long term exposure, the biological effectiveness of heavy ions is a matter for discussion (Ballarini et al. 2007; Cucinotta 2007).

The exposure of the human body to radiation is quantified by different types of radiation dose. Absorbed dose refers to the energy deposited by the radiation in part of or in the entire body and it is expressed in the units Gray (Gy) or rad ($1\ \mathrm{Gy} = 100\ \mathrm{rad} = 1\ \mathrm{J\,kg^{-1}}$). The dose equivalent is the sum of absorbed doses in the entire body due to different types of radiation, weighted by quality factors that quantify the biological effectiveness of each radiation type. The effective dose is the sum of the energies deposited by all types of radiation in different organs multiplied by weighting factors that are functions of both the type of radiation and the nature of the organ concerned. Both dose equivalent and effective dose are measured in Sievert (Sv) or in rem units ($1\ \mathrm{Sv} = 100$ rem). Quality and weighting factors for dose equivalent and effective dose are defined by the International Commission on Radiological Protection (ICRP 1990). Dose equivalent and effective dose induced by different types of primary particles have been calculated using Monte Carlo codes or deterministic models applied to rather sophisticated phantom models of the entire body (Ballarini et al. 2004; Cucinotta 2007). Flux to dose conversion factors are given by, e.g., ICRP (1993) and Pelliccioni (2000).

Although significant progress has been made in the last decades in the field of radiation biology, major uncertainty regarding the assessment of the radiation risk to humans still persists. The main reason for this is that the effect of a given type of radiation is quantified by the extrapolation of high dose data obtained mainly from nuclear bomb survivors who were principally exposed to particles with low linear energy transfer (LET). LET gives the energy loss of an ionizing particle per unit length of its track. LET decreases as a function of projectile speed and increases as a function of charge. Particles with high LET yield larger biological effects than those with low LET. For example, chromosome aberrations are most effectively produced by particles with an LET of $\sim$100 keV $\mu\mathrm{m}^{-1}$, corresponding to typical values for ions heavier than protons (e.g., Kawata et al. 2004). The reader will find more information on the biological effects of radiation in the reports of Ballarini et al. (2007) and Cucinotta (2007), and references therein.

2.3 Radiation Effects on Atmosphere

Energetic particles cannot penetrate the thick atmosphere of the Earth since they collide, typically in the lower stratosphere, with nuclei of atmospheric gases (mostly nitrogen and

oxygen), thereby initiating a cascade of secondaries (see Dorman 2004; Grieder 2001, and references therein). The cascade consists of three principal components: the "soft" or electromagnetic component including electrons, positrons, and photons; the "hard" or muon component; and the "hadronic" nucleonic component consisting mostly of suprathermal protons and neutrons. The cascade leads to notable physicochemical effects in the atmosphere. The most important effect is cosmic ray induced ionization (CRII) in the atmosphere. CRs form the principal source of ionization in the low and middle atmosphere, except in the near-to-ground layer, where natural radioactivity in the soil may play a role. Ionization of the upper atmosphere is dominated by solar UV-radiation and by precipitating, less energetic particles of interplanetary and magnetospheric origin. The permanent ionization of the atmosphere has numerous consequences for various aspects of the terrestrial environment, as discussed elsewhere (see, e.g., Bazilevskaya et al. 2008; Dorman 2004, and references therein).

CRs can also lead to chemical changes in the atmosphere (e.g., Chapter 13 in Dorman 2004; Section 4 in Kudela et al. 2000). Important for the terrestrial environment, particularly for climate, is the destruction of ozone (Thorne 1977; Baker et al. 1987) and the formation of minor atmospheric components (e.g., OH_x and NO_y) (Damiani et al. 2006; Jackman and McPeters 2004; Krivolutsky 2003). These changes can be quite dramatic during SEP events in the polar upper atmosphere (Verronen et al. 2006; Damiani et al. 2008; Jackman et al. 2008; Storini et al. 2008). High relativistic electron precipitation, induced by the solar wind-magnetospheric coupling during solar storms, is also able to affect the mesosphere and upper stratosphere (see, e.g., Randall et al. 2005; Orsolini et al. 2005). Nevertheless, the ionization rate from electrons should be less effective than the one expected from SEPs. Additionally, a small quantity of cosmogenic nuclides can be produced in the atmosphere as a result of CR nuclear interactions. Although their amount is negligible for chemical changes, the fact that GCRs constitute their only source, provides a unique opportunity to use these particles as tracers (Usoskin et al. 2009b). On a long-term scale, cosmogenic isotopes such as ^{14}C and ^{10}Be, measured in stratified natural archives, allow the reconstruction of solar activity over past millennia (Beer et al. 2006; Solanki et al. 2004). On a short-term scale, the use of short-living cosmogenic isotopes (e.g., ^{7}Be) makes it possible to monitor air mass dynamics (Koch et al. 1996; Raisbeck et al. 1981).

Overall, CRs, although they carry a negligible amount of energy to Earth, induce key physicochemical changes in the atmosphere and are partly responsible for stimulating long-term solar-terrestrial relationships (Usoskin and Kovaltsov 2008a).

3 Variability of the Particle Radiation Environment—Scientific Modeling

In this section, we will review efforts to scientifically model the physical processes that govern the dynamics of the Earth's particle radiation environment.

3.1 GCR Modulation

Transport of GCRs in the heliosphere leads to dynamical changes in their energy spectrum and anisotropy. This process is collectively called solar modulation. The theory of modulation is based on the transport equation (Parker 1965; Toptygin 1985):

$$\frac{\partial f}{\partial t} - \nabla \cdot (\mathbf{K}^{(S)} \cdot \nabla f) + \mathbf{V} \cdot \nabla f + \langle \mathbf{v}_D \rangle \cdot \nabla f - \frac{1}{3}(\nabla \cdot \mathbf{V}) \frac{\partial f}{\partial \ln p} = Q, \tag{1}$$

where $f(r, p, t)$ is the omnidirectional distribution function of GCRs, p the particle's momentum, r the heliocentric distance, $\mathbf{V}$ the solar wind velocity, $\mathbf{K}^{(S)}$ the symmetric part of the diffusion tensor, $\langle \mathbf{v}_D \rangle$ the pitch-angle averaged guiding center drift velocity, and Q is the CR source function. It describes the main transport processes: diffusion of particles due to their scattering off magnetic inhomogeneities; convection in the out-streaming solar wind; drifts of two types: the gradient-curvature drift in the regular heliospheric magnetic field and drift along the heliospheric current sheet; and adiabatic energy losses in the expanding solar wind. These processes are defined by the geometrical structure, polarity, strength and the level of turbulence in the IMF and solar wind, which are ultimately driven by variable solar activity. This leads to temporal variability of the modulation on different time scales. The full solution of (1) requires sophisticated 3-D numerical modeling (Kota and Jokipii 1983; Kota 1995). Unfortunately, many parameters (e.g., the diffusion tensor, see Burger and Hattingh 1998) cannot be measured or even independently evaluated. Therefore, one needs to compromise between limited input information and reality through introducing reasonable simplifications in the full theory, keeping only the most important features and sacrificing minor effects.

At time scales longer than the solar rotation period (i.e., 27 days), it is usual to reduce the problem to that of a 2D quasi-steady case by assuming azimuthal symmetry (Alanko-Huotari et al. 2007; Jokipii and Kopriva 1979; Langner et al. 2006). The additional assumption of a spherically symmetric heliosphere reduces the problem to a 1D case (Caballero-Lopez and Moraal 2004; Fisk and Axford 1969; Usoskin et al. 2002a), but this eliminates the drift effect and can hardly serve as a valid physical model. Nevertheless, its simplified version, the so-called *force-field* approximation (Caballero-Lopez and Moraal 2004; Gleeson and Axford 1968), can describe with reasonable precision the differential energy spectrum of GCRs near Earth. In the framework of this approximation, the energy spectrum of i-th GCR species (with charge Z_i and mass A_i numbers) at 1 AU, J_i, is related to the unmodulated local interstellar spectrum (LIS) of the same species, $J_{\mathrm{LIS},i}$, via the modulation potential ϕ as:

$$J_i(T, \phi) = J_{\mathrm{LIS},i}(T + \Phi_i) \frac{T\,(T + 2T_\mathrm{r})}{(T + \Phi_i)(T + \Phi_i + 2T_\mathrm{r})}, \tag{2}$$

where T is the particle's kinetic energy per nucleon, $\Phi_i = (eZ_i/A_i)\phi$, and $T_\mathrm{r} = 0.938$ GeV/nucl. The only temporal variable here is ϕ, which is related to solar activity. Equation (2) includes also the function J_LIS, the exact shape of which is not known (Burger et al. 2000; Garcia-Munoz et al. 1975; Moskalenko et al. 2002; Webber and Higbie 2003). Here we use the LIS of protons in the form (Burger et al. 2000; Usoskin et al. 2005):

$$J_\mathrm{LIS}(T) = \frac{1.9 \times 10^4 \cdot P(T)^{-2.78}}{1 + 0.4866\, P(T)^{-2.51}}, \tag{3}$$

where $P(T) = \sqrt{T\,(T + 2\,T_\mathrm{r})}$, J and T are expressed in units of particles/(m^2 sr s GeV/nucl) and in GeV/nucl, respectively.

The GCR spectrum above 200 MeV/nucl near Earth can be fitted by (2) using a single parameter (ϕ) pertaining to a wide range of solar activity levels (see Fig. 1). We note that while ϕ formally represents the mean energy loss of a CR particle inside the heliosphere, it comprises only a formal spectral index whose physical interpretation is not straightforward, especially on short time scales and in relation to periods of elevated solar activity. Since the absolute values of ϕ obtained using different models for the LIS may differ from each other, mutual scaling is needed in order to compare them. For example, the modulation potential

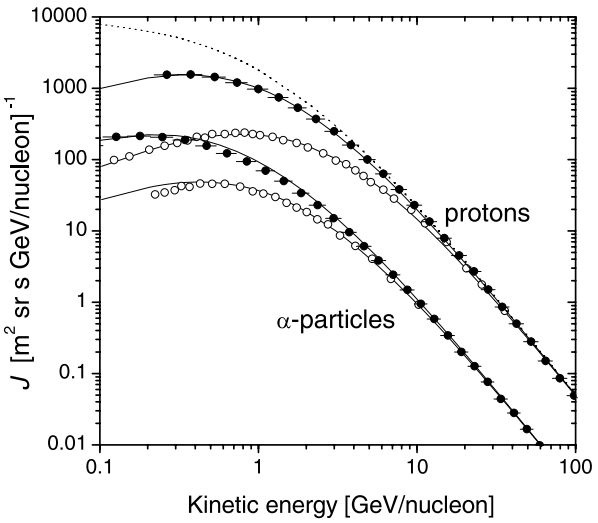

Fig. 1 Energy spectra of the two components of GCRs: protons (*upper curves*) and α-particles (*lower curves*). *Filled* and *open circles* depict the results of direct measurements made during a quiet period in June 1998 (Alcaraz et al. 2000a, 2000b) and an active period in September 1989 (Webber et al. 1991), respectively. The *curves* depict the best fit model results with $\phi = 530$ MV and $\phi = 1350$ MV, respectively (Usoskin et al. 2005). The *dotted curve* corresponds to the LIS ($\phi = 0$) for protons (Burger et al. 2000)

ϕ_{CL} obtained in the framework of the often used model by Castagnoli and Lal (1980) can be compared with that obtained by (2) and (3) as $\phi_{\mathrm{CL}} = 0.97\phi - 78$ MV (Usoskin et al. 2005).

The force-field approximation is widely used in various applications concerning the Earth's radiation environment, e.g., determining CR induced ionization (Pallé et al. 2004; Usoskin and Kovaltsov 2006), the production of cosmogenic isotopes (Masarik and Beer 1999; Webber et al. 2007; Usoskin and Kovaltsov 2008b), and solar activity reconstructions (Beer et al. 2006; Solanki et al. 2004). It is important to recognize that the value of ϕ is the same for all GCR species. The most abundant GCRs are protons and α-particles. While the fraction of α-particles in GCR number density is small, the contribution they make to the Earth's radiation environment is important. Due to their smaller Z/A ratio, they are less influenced than are protons by heliospheric modulation and by geomagnetic shielding. The relative contribution of α-particles greatly increases with decreasing energy, reaching up to 30–50% of the total GCR radiation effect (Usoskin and Kovaltsov 2006).

The observable variability of GCRs (Fig. 2) can be roughly divided into three time scales, each attributable to different effects. On short time scales (days) most important are the brief suppressions of GCRs (up to 30% during several days) called Forbush decreases, which are caused by transient, propagating/corotating interplanetary perturbations passing through near-Earth space. GCR modulation on a longer time scale is dominated by the 11-yr cycle. On yet longer time scales (centennia to millennia) solar activity and slow geomagnetic variations each play a role.

CR intensity has been continuously monitored by the world-wide neutron monitor (NM) network since 1951. Using a full analysis of these data, the values of ϕ were computed (see Usoskin et al. 2005, and http://cosmicrays.oulu.fi/phi/), as shown in Fig. 2a. This result is in good agreement with data from occasional direct balloon and space-borne measurements of the CR spectrum. Although direct CR measurements (McCracken and Beer 2007) do not extend far back in time, indirect methods can be used to obtain information over a considerably longer time scale. Figure 2b presents a set of reconstructions of the modulation potential since 1700 AD, including a model computation (Usoskin et al. 2002b) from sunspot numbers and reconstructions from cosmogenic isotopes ^{14}C (Usoskin et al. 2006, 2007) and ^{10}Be in polar ice cores (McCracken et al. 2004;

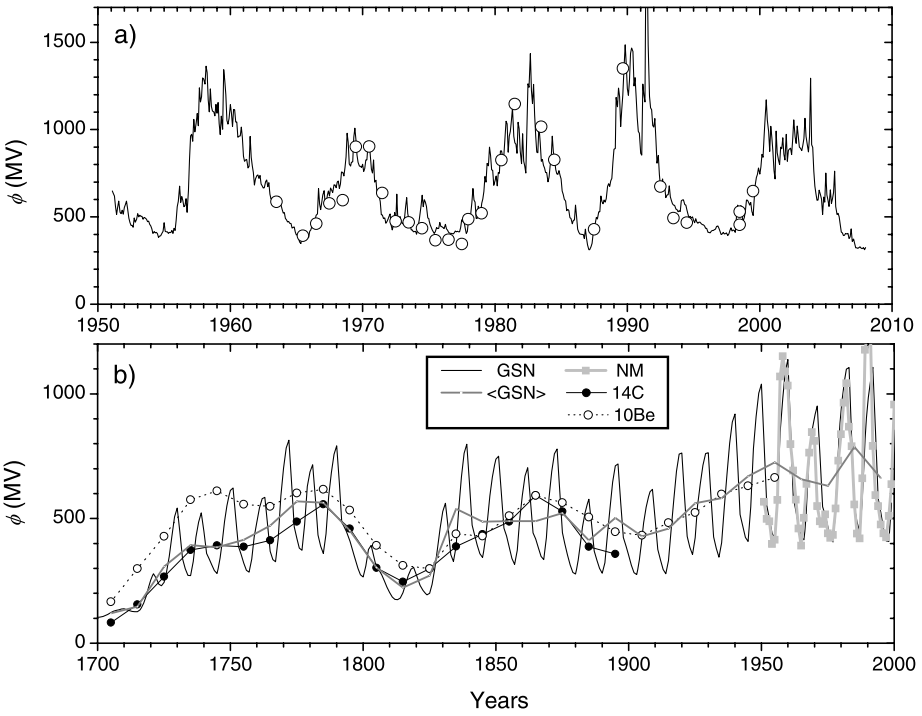

Fig. 2 Temporal variations of the modulation potential ϕ. **a**) Based on the data of the NM network (Usoskin et al. 2005). *Dots* correspond to direct balloon- or space-borne in-situ measurements of the GCR energy spectrum. **b**) Reconstruction using different methods: from group sunspot numbers (yearly "GSN" curve and cycle-averaged "⟨GSN⟩" curve) according to Usoskin et al. (2002b); the same as in panel a) but annually averaged ("NM" curve); from ^{14}C data in tree rings (decadal "14C" curve) (Usoskin et al. 2006, 2007); from ^{10}Be data in polar ice cores (decadal "10Be" curve) (McCracken et al. 2004)

Vonmoos et al. 2006). All the reconstructions agree with regard to their main features, viz. a weak modulation during the Maunder minimum followed by a period of moderate modulation until 1900 (with the Dalton minimum ca. 1820). The modern modulation ($\langle\phi\rangle = 680$ MV for 1951–2007) is significantly higher than that for the last centennia (380–470 MV) and millennia (390–460 MV), in agreement with independent estimates that the present-day IMF is unusually strong (Beer et al. 2006; Lockwood et al. 1999; Solanki et al. 2000, 2004; Usoskin et al. 2007).

3.2 Particle Acceleration at the Sun and Transport in the Heliosphere

Particle acceleration to the highest energies (i.e., beyond 1 MeV for protons and 100 keV for electrons) occurs at the Sun during flares and CMEs (e.g., Reames 1999). The acceleration processes draw their energy from magnetic energy stored in the solar corona, which is released as thermal and kinetic energy and radiation. SEP events can be roughly divided into two classes, impulsive and gradual, according to the time scales of their associated particle flux variations (Reames 1999). Impulsive SEP events, which last from a few hours to days, are related to impulsive flares, are enriched in electrons, ^{3}He and heavy ions, and have ion charge states typical of high-temperature plasma. Gradual SEP events, which last from a few

days to a week, are related to CMEs and to gradual flares and exhibit "normal" coronal abundances and charge states. Gradual events generally display larger proton fluences and peak fluxes than do impulsive events, so they may be regarded as being more important from the point of view of the radiation environment. However, the clear-cut separation of gradual and impulsive events has become somewhat blurred over the most recent decade by the observations of hybrid events showing large fluxes and fluences typical for gradual events but ion abundances more typical of flares (e.g., Tylka et al. 2005; Cane et al. 2006). Thus, it is very important to understand particle acceleration in flares as well as in CMEs. Two competing ideas to explain hybrid events have been presented: (i) that the flare-like particle abundances and charge states are due to a direct flare component in the particle distribution (Cane et al. 2006); and (ii) that the abundances result from re-acceleration of suprathermal flare particles (left behind from previous flares or made available from the accompanying flare) by a coronal shock propagating nearly perpendicular to the ambient magnetic field (Tylka et al. 2005; Sandroos and Vainio 2007).

It is generally accepted that gradual events are accelerated in shocks driven by CMEs through the diffusive shock acceleration mechanism (see, e.g., Reames 1999, and references therein). Ion acceleration mechanisms operating in impulsive events are still under discussion. Stochastic acceleration by high-frequency plasma waves is currently the only model able to explain the abundance enhancements of minor ions observed in impulsive events (Liu et al. 2004). Mechanisms of electron acceleration are presently debated, and proposed models range from shock drift acceleration (Mann et al. 2006) to acceleration by DC electric fields prevailing in reconnecting current sheets (Litvinenko 2003).

Particle transport through the interplanetary medium is governed, in principle, by the same physical processes that are responsible for the modulation of GCRs. However, because of the pronounced short-scale temporal variability of the source, the diffusion approximation (based on the assumption of quasi-isotropic particle distributions) underlying the modulation equation is not any longer deemed to be valid. Thus, SEP transport is generally treated using the so-called focused transport equation, which, in the simplest case of negligible convection and adiabatic deceleration (Roelof 1969; Ruffolo 1991), is given by

$$\frac{\partial f}{\partial t} + \mu v \frac{\partial f}{\partial s} + \frac{1-\mu^2}{2L} v \frac{\partial f}{\partial \mu} - \frac{\partial}{\partial \mu}\left(D_\mu \frac{\partial f}{\partial \mu} \right) = Q, \tag{4}$$

where $f(s, v, \mu, t) = \mathrm{d}^6 N/(\mathrm{d}^3 x\, \mathrm{d}^3 p)$ is the distribution function of the SEPs on a given magnetic field line, s is the coordinate measured along the magnetic field, v is particle speed, μ is the cosine of pitch angle (with $\mu = 1$ denoting outward propagation), $L = -B/(\partial B/\partial s)$ is the focusing length determined by the mean magnetic field, $B(s)$, as a function of distance, $D_\mu = \frac{1}{2}\langle(\Delta\mu)^2\rangle/\Delta t$ is the pitch-angle diffusion coefficient, and $Q = Q(s, v, \mu, t)$ is the source function, determined by the processes that accelerate particles in the solar corona and solar wind. Later versions of the focused transport equation have included the effects of adiabatic energy changes and convection (Ruffolo 1995) and partly even the effects of drift motions due to field inhomogeneities (le Roux et al. 2007). These inclusions are necessary if the energy changes of the energetic particles in the solar wind, including particle acceleration in interplanetary shock waves, are taken into account.

The most important unknown parameter in the focused transport equation is the pitch-angle diffusion coefficient. Usually, this parameter, $D_\mu = \frac{1}{2}(1-\mu^2)\nu(v, \mu, s)$, is modeled by choosing the scattering frequency, $\nu \equiv \langle(\Delta\alpha)^2\rangle/\Delta t$ (where $\alpha = \arccos\mu$), to be in the form of a power law $\nu = A(v, s)|\mu|^{q-1}$. The power-law index is determined by the spectral index, q, of the intensity of magnetic field fluctuations, $I(k) = I_0|k_0/k|^q$, through quasi-linear theory (Jokipii 1966). The magnitude, $A = \pi\Omega(k_0 I_0/B^2)|k_0 v/\Omega|^{1-q}$, is related to the

particle gyrofrequency Ω and to the intensity I_0 of the magnetic fluctuations at a reference wavenumber, k_0, but since the intensity is not known as a function of distance throughout the inner heliosphere modelers usually fix A by introducing the parallel mean free path, $\lambda_\parallel$, through

$$\lambda_\parallel \equiv \frac{3v}{4}\int_{-1}^{+1}\frac{1-\mu^2}{\nu}\mathrm{d}\mu = \frac{3v}{A(2-q)(4-q)}, \tag{5}$$

and adopting a spatial dependence for this parameter. The dependence of the mean free path on rigidity ($R = pc/Q$, where Q is the particle charge and c is the speed of light) is usually taken to be fixed by the spectral index q as $\lambda_\parallel \propto R^{2-q}$ in conformity with the quasi-linear result.

The focused transport equation cannot be solved analytically in any realistic magnetic field geometry. Several simulation codes exist, however, to provide numerical solutions, and they incorporate two main types of solvers: (i) finite difference (FD) schemes (e.g., Ruffolo 1991, 1995; Lario et al. 1998) and (ii) Monte Carlo (MC) simulations (e.g., Kocharov et al. 1998; Vainio et al. 2000; Agueda et al. 2008). In FD schemes, one solves the focused transport equation directly on a grid, and in MC simulations one traces individual particles that follow the stochastic equations of motion equivalent to the focused transport equation. Both numerical methods have attractive features as well as some drawbacks. The FD schemes are numerically very efficient and provide the solution very rapidly for smoothly-behaved initial and boundary conditions, but they are not suited for the δ-function-like particle injections used in computing Green's functions of particle transport. The MC schemes, on the other hand, are very easy to implement and update, because including a physical transport or acceleration process in the model usually only requires the addition of a few lines of additional code. They can also easily handle any initial conditions and any boundary conditions that can be specified on a microscopic level (i.e., as rules of particle behavior at the boundaries of the simulation). As a downside, however, MC simulations usually require a large amount of CPU time to collect sufficient statistics for the reconstruction of particle distributions.

One of the most serious complicating factors in SEP transport and acceleration at shock waves is that the wave–particle interactions responsible for particle acceleration lead also to the modification of turbulent fluctuations in the ambient medium. In the simplest approach to studying plasma turbulence, the fluctuating fields are treated as linear wave modes and, in this way, it is possible to determine the growth rates of the waves from the particle distributions using quasi-linear theory. This idea has so far been applied to a coupled system of energetic protons and Alfvén waves (Ng and Reames 1994, 2008; Rice et al. 2003; Vainio 2003; Lee 2005; Vainio and Laitinen 2007; Vainio and Laitinen 2008) and modeling efforts show that non-linear models that include the dynamics of coronal and interplanetary turbulence are required in order to provide a consistent picture of particle transport and acceleration during the largest, space-weather relevant, SEP events. Furthermore, in addition to particle transport and acceleration conditions, models must also be able to provide a description of the dynamics of CME-driven shocks. This requires integrating a global MHD simulation with particle transport and acceleration simulations. First steps in this direction have already been taken using a test-particle code (see, e.g., Giacalone and Kóta 2006, and references therein), but successful integration of a fully self-consistent particle simulation with an MHD code has not yet been reported. (See, however, Zank et al. 2007, and included references.) It is presently difficult to estimate when such complex models will be mature enough for engineering applications. That is why test-particle models with their transport conditions tuned to reproduce individual SEP events continue to remain important tools for space weather applications at least until the nearest future. One example of such a tool is

SOLPENCO developed by the University of Barcelona (see Waterman et al. 2009 and references therein).

3.3 Magnetospheric Transmission of Solar and Galactic CRs

The Earth's magnetosphere presents a shield against GCRs and SEPs (the latter are also referred to as solar cosmic rays, SCRs). The transmission of CRs through the magnetosphere is quantified by the so-called cutoff rigidity, which represents roughly the lowest rigidity limit in the spectrum of particles reaching a given position from a given direction (Cooke et al. 1991).

For the study of solar energetic particles observed on Earth during ground level enhancements (GLEs; Forbush 1946) and for the study of CR anisotropy, it is important to determine the asymptotic direction of a CR particle, which represents its direction of motion before entering the magnetosphere. Cutoff rigidities and asymptotic directions of incidence are computed by using backward trajectory tracing codes, which combine an internal model of the Earth magnetic field and a magnetospheric magnetic field model (Bobik et al. 2003; Smart et al. 2000; Flückiger and Kobel 1990). In these codes the trajectories of CRs arriving at the same observing position and from the same direction of incidence, are computed backward in time for a set of rigidities spanning a large range of values having a constant rigidity interval δR (usually 0.01 GV). In such computations three rigidity regions are identified: (i) a high rigidity region where all trajectories escape the magnetosphere (allowed trajectories); (ii) a low rigidity region where none of the trajectories escape the magnetosphere (forbidden trajectories); (iii) an intermediate penumbral region where bands of allowed trajectories are separated by bands of forbidden ones. The lowest rigidity in the high rigidity region is called the upper cutoff rigidity R_U. The lowest rigidity in the penumbra is called the lower cut-off rigidity R_L. Finally, the effective cutoff rigidity R_C is given by $R_C = R_U - n\,\delta R$, where n represents the number of allowed trajectories in the penumbra. The reader will find a complete description of the asymptotic direction computation method as well as CR cutoff terminology in Cooke et al. (1991).

For the analysis of the measurements of most ground-based CR experiments, where mostly vertically incident particles contribute to the counting rate, it is usually assumed that only CRs with rigidity higher than the vertical effective cutoff rigidity R_C can reach the top of the Earth's atmosphere from all directions of incidence. However, at high altitudes and for positions with high cutoff rigidity or in space, the contribution of non-vertical particles becomes important and the variation of R_C with the direction of incidence must be taken into account (Clem et al. 1997; Dorman et al. 2008). The effective cutoff rigidity gives only a rough approximation of the complex structure of the penumbra. Various authors have treated the geomagnetic transmission in the penumbral region more precisely than just by using R_C (Boberg et al. 199; Kudela and Usoskin 2004; Kudela et al. 2008; Smart et al. 2006).

The particle cutoff rigidity and asymptotic direction of incidence vary on different time scales in association with variability in the geomagnetic field. Secular variations in the geomagnetic field produce long-term variations in the cutoff. A diurnal variation in the geomagnetic cutoff is due to the rotation of the Earth inside the magnetosphere that is aligned with the solar wind flow direction.

Geomagnetic transmission also depends strongly on the level of geomagnetic activity. Different authors have studied the variation in cutoff rigidity as a function of substorm and storm activity. Flückiger et al. (1981, 1990) investigated the dependence of cutoff rigidity on magnetospheric current systems during magnetic storms. Smart et al. (1999) calculated

the changes in vertical R_C as a function of magnetic activity. Belov et al. (2005) and Tyasto et al. (2008) studied variation in vertical R_C that occurred during a big magnetic storm in November 2003. Kudela et al. (2008) and Desorgher et al. (2009) examined the variation of geomagnetic transmissivity and asymptotic direction during major magnetic storms using different magnetic field models.

A significant limiting factor with regard to the precision achieved by magnetospheric transmission codes is the accuracy of the available magnetic field models. Over the last two decades, models of the Earth's magnetospheric magnetic field have been continuously improved to describe more precisely different contributing magnetospheric current systems and their time variation during magnetic storms (see, e.g., McCollough et al. 2008). Recently Desorgher et al. (2009) compared the different Tsyganenko models (Tsyganenko 1989, 1995, 1996; Tsyganenko and Sitnov 2005) and the Alexeev and Feldstein 2000 model (Alexeev et al. 1996; Alexeev and Feldstein 2001). They investigated the level of difference that is to be expected in computations of the radiation dose at aircraft altitude during GLEs when different magnetic field models are used to estimate geomagnetic transmission. They also compared the computed effective dose in the Earth's atmosphere produced by SEPs and GCRs at 06:55 UT during the 20 January 2005 GLE as estimated using different magnetic field models. The results of their calculations are presented in Fig. 3. The upper panel represents the computed radiation dose at 300 g/cm^2 atmospheric depth (altitude of about 9.1 km) obtained by using the Tsyganenko (1989) model. The same general pattern was obtained using all the models but significant local differences were present amongst them, as can be seen in the left bottom panel, due to differences in the asymptotic direction (plotted in the form of pitch angles in the right-hand panel). Desorgher et al. (2009) also investigated the possibility to test the magnetic field models during major magnetic storms through using NM data and they also studied the effect of individual magnetospheric currents on variations in cutoff rigidity.

When studying the long term influence of CRs on the Earth's environment, it is important to take into account the variation in the geomagnetic field that took place in the past. Barraclough (1974) published spherical harmonic models of the geomagnetic field for eight epochs between 1600 and 1910. By computing vertical cutoff rigidity using these models, Shea and Smart (2004) estimated that the decrease in the geomagnetic field over the last 400 years has probably given rise to a 10% increase in the CR flux on Earth. Archeomagnetism, sediments, volcanic data, and/or cosmogenic radionuclide data have been used by several authors to quantify the variation in the internal geomagnetic field on a millennium time scale (McElhinny and Senanayake 1982; Yang et al. 2000; Wagner et al. 2000; Muscheler et al. 2005; Laj et al. 2000, 2002). In most of the methods used to reconstruct the past geomagnetic field, the Earth's magnetic field was considered to be a geocentric dipole and the non-dipole component was neglected. The importance of the non-dipole component when quantifying the geomagnetic shielding during the past has been discussed by Flückiger et al. (2003) and Shea and Smart (2004). Recently, Korte and Constable (2005) released the first spherical harmonic model of the geomagnetic field for an interval extending from 7000 years in the past to the present day. By using this model Usoskin et al. (2008) showed that a variation in the tilt of the eccentric geomagnetic dipole leads to a significant regional variation in CRII on centennial and millennium time scales. Lifton et al. (2008) used the same model to compute, for the last 7000 years, grids of effective cutoff rigidity and used them in a study of time integrated distributions of in situ cosmogenic nuclide production rates. The most recent model (Genevey et al. 2008) provides an updated paleomagnetic reconstruction over the last millenia.

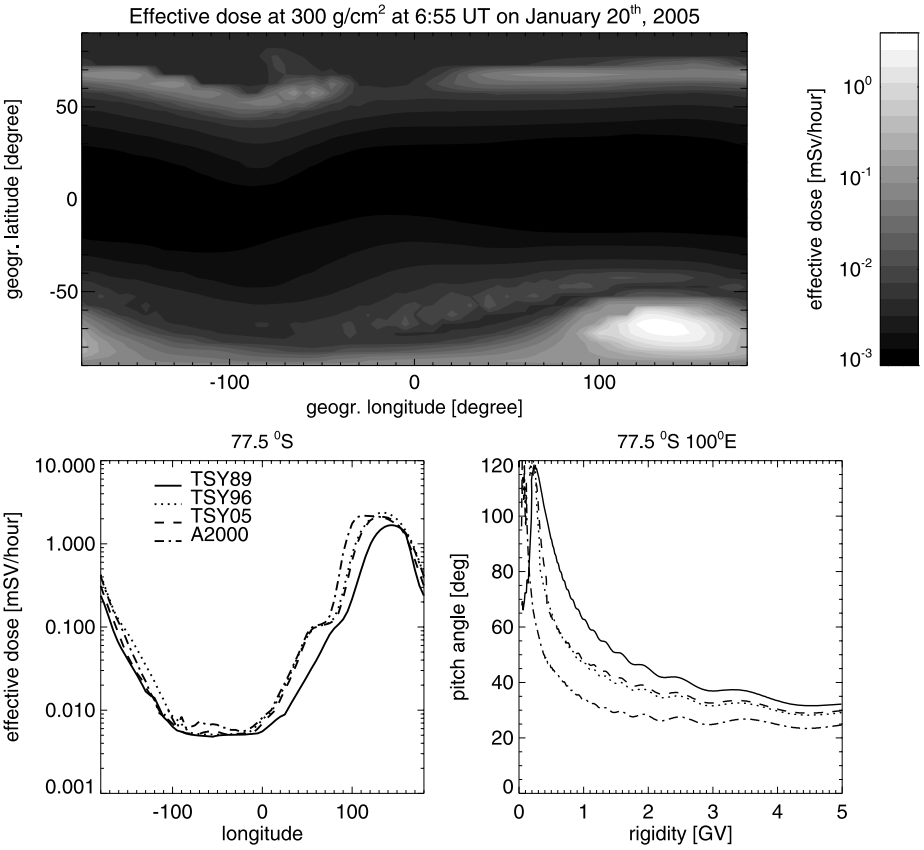

Fig. 3 The *top panel* represents the computed world map of radiation dose at 300 g/cm^2 (altitude of about 9.1 km) induced by SEPs and GCRs at 06:55 UT during the GLE of January 20, 2005. For these results the asymptotic directions of vertical incidence used for computing the flux of solar particles at the top of the atmosphere have been obtained by using the Tsyganeko89 model. The *lower left panel* represents the variation of the computed effective dose at 300 g/cm^2 for 77.5° south latitude as a function of longitude obtained by considering the Tsyganenko (1989) (*solid line*), Tsyganenko (1996) (*dotted line*), Tsyganenko and Sitnov (2005) (*dashed line*), and Alexeev and Feldstein 2000 (*dashed dotted line*) models. In the lower right panel, the pitch angle of the asymptotic direction of vertical incidence for the 77.5° south latitude and 100° east longitude position obtained with the same models is plotted as a function of rigidity

3.4 Atmospheric Effects of CRs

Ionization by GCRs is always present in the atmosphere, and it changes with the 11-year solar cycle due to solar modulation (Sect. 3.1). Although the ionizing effect of CRs has been known for a long time and led Victor Hess to discover CRs in 1912, reliable quantitative models of CRII (see below) have only appeared in the last decade. The first models were based on an analytical approximation of the atmospheric cascade (O'Brien 2005). Modern models are based on a full Monte Carlo simulation of the atmospheric cascade, including all the secondaries (Desorgher et al. 2005; Usoskin et al. 2004; Usoskin and Kovaltsov 2006; Velinov and Mishev 2007). Presently, two basic Monte-Carlo-based CRII models are commonly used. One is the Bern model (ATMOCOSMICS/PLANETOCOSMICS code—see Desorgher et al. 2005, Scherer et al. 2006), which is based on the Geant4 Monte Carlo

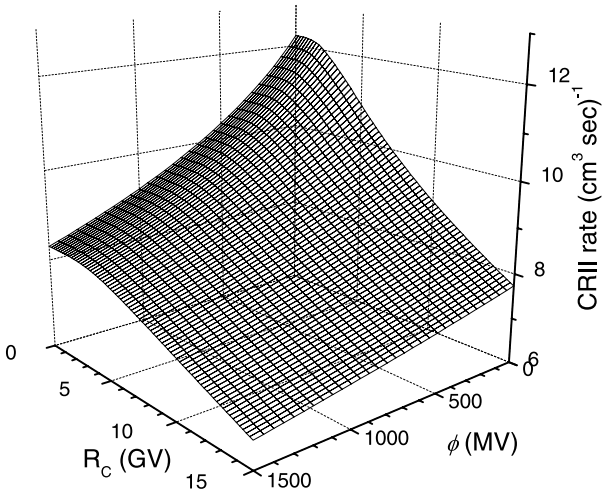

Fig. 4 CRII rate, computed by the Oulu model (Usoskin and Kovaltsov 2006) at the atmospheric depth 500 g/cm^2 (pressure 490 hPa, altitude of about 5.7 km) as a function of the geomagnetic cutoff rigidity R_C and modulation potential ϕ

simulation package. Another model is based on the CORSIKA+FLUKA Monte Carlo package and has been primarily developed as the Oulu CRAC (Cosmic Ray Atmospheric Cascade) model (Usoskin et al. 2004; Usoskin and Kovaltsov 2006). Similar approach has been later adopted by other groups (Velinov and Mishev 2007; Alexandrov et al. 2008; Vasilyev et al. 2008). Note that ionization of the upper atmosphere, where the cascade is not developed, is well described by an analytical model (Velinov and Mateev 2008). For a detailed review of the above models see Usoskin et al. (2009a).

CRII in the atmosphere is defined by three parameters: altitude—ionization increases with altitude, reaches maximum at about 15 km and, thereafter, decreases again; local geomagnetic shielding, which is usually quantified via the geomagnetic cutoff rigidity R_C (Cooke et al. 1991)—the ionization rate is highest at the geomagnetic poles and less at the equator (R_C at a given geographical location may change with time due to secular changes in the geomagnetic field); and, finally, the time variability of CRII by the variable heliospheric modulation, which is quantified via the modulation potential ϕ. An example of the CRII rate at an atmospheric depth of 500 g/cm^2 (altitude of 5.7 km) as a function of R_C and ϕ is shown in Fig. 4, where the range of variations is seen to achieve a factor of 2 between the polar atmosphere at solar minimum (low R_C; low ϕ) and the equatorial atmosphere at solar maximum (high R_C; high ϕ).

The range of validity of the CRII models has been studied by Usoskin et al. (2009a). Figure 5 shows a comparison between the CRII simulation results and direct balloon-borne measurements of the ionization rate for two cases, bounding the possible range in the CRII rate: the polar atmosphere during a solar minimum (panel a) and the equatorial atmosphere (panel b). The models agree with the measured data and with each other within 20% beneath the middle stratosphere, suggesting that the models adequately reproduce CRII in the whole range of solar modulation (see also Usoskin and Kovaltsov 2006). The slight excess of the measured ionization rate over the computed one in the upper stratosphere (above 25–30 km, see Fig. 5a) can be attributed to the action of ionization agents other than GCRs (Bazilevskaya et al. 2008).

In addition to the permanent flux of GCRs, sporadic SEP events (Sect. 3.2) may lead to an important increase in atmospheric ionization. While the ionization effect of SEP events is usually limited to the upper polar atmosphere, extreme SEP events may produce ionization

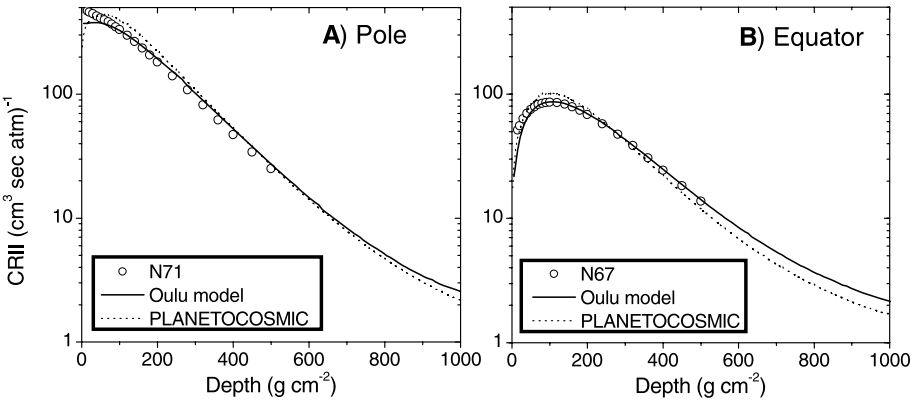

Fig. 5 CRII rate at the pole (panel **a**) and equator (panel **b**) during the solar minimum. *Curves* depict computations using the Oulu (Usoskin and Kovaltsov 2006) and PLANETOCOSMICS (Desorgher et al. 2005) models. Dots represent direct measurements by Neher (1967), labeled N67 and Neher (1971, labeled N71)

at lower altitudes. Bütikofer et al. (2008a) studied the ionization effect for the severe SEP event of 20 January 2005, which was one of the strongest GLEs ever observed. In contrast to GCRs, which impinge on Earth nearly isotropically, SEPs have an anisotropic distribution, especially during the main phase of the event when they propagate mostly along the IMF lines. This results in greatly enhanced (by two orders of magnitude) ionization in the troposphere in the Antarctic region during the peak of the event. (The ionization pattern closely resembles the dose rate pattern presented in Fig. 3.) This may lead to physicochemical consequences in the middle- and upper polar atmosphere. The ionization effect of SEP events is local and is most important in the polar atmosphere. The global effect of SEP induced ionization is tiny, even in the case of severe events (Bazilevskaya et al. 2008).

3.5 Radiation Belts

3.5.1 Trapped Protons

The proton radiation belt contains some of the most penetrating particles found in all the radiation belts (energies exceed 100 MeV). The location of the proton belt varies with energy, with the peak flux of >50 MeV protons near $L = 1.3$, while the flux at lower energies peaks at more outward L shells. Due to a weakness in the magnetic field in the South Atlantic (South Atlantic Anomaly) these particles (as well as electrons) penetrate deeper into the terrestrial atmosphere in this region. Consequently, they pose a particular hazard to satellites in LEO at that location.

There are three main processes that contribute to the formation of the proton belt. CRAND is mainly responsible for energies >100 MeV (White 1973). In the CRAND process a fraction of the cosmic ray flux incident on the atmosphere is backscattered as neutrons which subsequently decay into protons and electrons. Direct entry and trapping of solar protons during solar proton events and geomagnetic storms provides a second source of protons (Hudson et al. 1995; Kress et al. 2005), and inward transport of protons across the magnetic field towards the Earth by radial diffusion contributes a third source, which is effective in the outer zone $L > 1.7$ (Albert et al. 1998; Albert and Ginet 1998). These sources are balanced by losses due to Coulomb collisions

with electrons in the plasmasphere, charge exchange with Hydrogen atoms, and atmospheric absorption.

The inner part of the proton belt, $L < 1.7$, is very stable. Over hundreds of years, secular changes in the Earth's magnetic field may gradually increase the proton intensity by a factor of 10 due to contracting drift shells (Selesnick et al. 2007). The current reduction in the Earth's magnetic field and movement of the South Atlantic Anomaly region are, therefore, of importance when planning future satellite designs and orbits. On timescales of the order of the 11-year solar cycle, high solar activity causes heating and expansion of the upper atmosphere, which, in turn, increases the collision rate and proton losses at a fixed altitude. Consequently, the proton flux displays a solar cycle variation that is in anticorrelation with the solar flux (Miyoshi et al. 2000). However, the most dramatic variations in the proton belt occur in the outer region $L > 2$ and have been observed during the interaction of an interplanetary shock with the Earth's magnetosphere. For example, during an event on 24 March 1991 a new proton belt was formed within 3 minutes (Blake et al. 1992). Shock-related compression of the magnetosphere was able to accelerate protons of solar origin up to energies of tens of MeV on timescales of tens of seconds (Hudson et al. 1995). A similar shock compression acceleration event was observed in July 2000 (Looper et al. 2005; Lorentzen et al. 2002) when the presence of iron suggested a solar wind source, whereas the timings of other events are more consistent with inward radial diffusion (Lorentzen et al. 2002). Dynamic models of the proton radiation belt are now well developed (Vacaresse et al. 1999; Selesnick et al. 2007), but they still require work in order to reproduce the variability of the outer region $L > 1.7$.

3.5.2 Trapped Electrons

Electron flux variations in the radiation belts are a result of an imbalance between acceleration, transport and loss processes (see, e.g., the recent reviews by Shprits et al. 2008a, 2008b).

Electron Acceleration. It has been established that electron acceleration occurs inside the magnetosphere (Li et al. 1997) and several possible acceleration mechanisms have been proposed (see the reviews by Li and Temerin 2001; Friedel et al. 2002; Horne 2002). Until recently betatron and Fermi acceleration as a result of transport across the magnetic field (radial diffusion) towards the Earth has constituted the most widely accepted theory of electron acceleration. This process is much more efficient when ULF waves at frequencies of a few Hz are present (Elkington et al. 1999), and there is a high correlation between the occurrence of ULF waves, flux increases, and the speed of the solar wind (Mathie and Mann 2000). In order to diffuse electrons towards the Earth the electron phase space density must increase with increasing L. However, recent observations and re-analysis studies have shown that the particle phase space density peaks in the inner region near $L = 4.5$ and not in the outer region as required by inward radial transport (Green and Kivelson 2004; Iles et al. 2006; Chan et al. 2007; Shprits et al. 2007). This suggests that a local acceleration mechanism is present, thereby changing our concept of how the radiation belts are formed (Horne 2007).

Acceleration through wave-particle interactions is the leading candidate mechanism for providing local acceleration (Horne and Thorne 1998; Summers et al. 1998). In this theory, waves at frequencies comparable to the electron cyclotron frequency resonate with the electrons via Doppler shifted cyclotron resonance. This process breaks the first, and therefore all three, adiabatic invariants. There are five different wave modes that could contribute to local acceleration, but the most promising candidate so far is whistler mode chorus waves (Horne

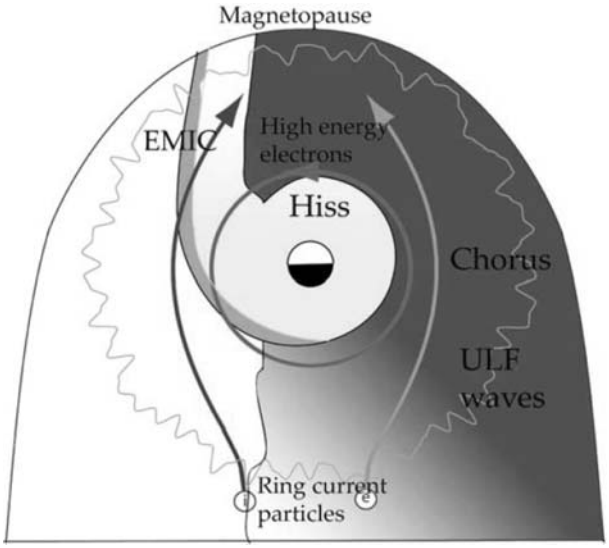

Fig. 6 Schematic diagram showing the regions in MLT where different types of waves can scatter relativistic electrons through resonant interactions. The *light* and *dark gray lines* show the convection of injected ring current electrons and ions. The *gray-shaded regions* show different types of waves which scatter electrons via Doppler shifted cyclotron resonance, and the *wavy lines* refer to ULF waves. After Shprits et al. (2006a)

and Thorne 1998; Horne et al. 2003a, 2003b, 2005a, 2005b, 2006; Shprits et al. 2006a, 2006b; Summers et al. 1998, 2004). In this theory a source of low energy electrons (∼10 keV) from the plasma sheet is injected into lower L shells by convective (and inductive) electric fields during substorms. These particles form the seed population. As the particles are injected into regions of higher magnetic field strength an anisotropic distribution develops, peaked perpendicular to the magnetic field, which excites whistler mode waves via Doppler shifted cyclotron resonance (See Fig. 6, after Shprits et al. 2006a). The waves grow by scattering low energy (∼10 keV) electrons at small pitch angles into the atmosphere, but, at the same time, they are able to resonate with, and scatter, much higher energy electrons at large pitch angles that remain trapped inside the magnetic field. In effect there is a transfer of energy from a large number of low energy electrons at small pitch angles to accelerate a fraction of the population at large pitch angles to higher energies. Provided that the wave power is enhanced for a sufficient amount of time, electrons can be diffused to higher energies and produce a net increase in flux.

Over the last few years several pieces of research have supported the idea of wave-related acceleration. First, chorus wave power is most intense between $L = 4$–6 from midnight MLT, through dawn to the early afternoon sector, corresponding to the peak of the outer radiation belt. Second, chorus wave power increases with magnetic activity outside the plasmasphere (Meredith et al. 2000, 2001, 2003a, 2003b, 2003c) in regions where the ratio of the electron plasma frequency to the electron gyrofrequency is low, which is the condition required for efficient electron diffusion to higher energies (Horne et al. 2003b). Third, wave acceleration predicts 'flat top' pitch angle distributions that are flat between about 60–90 degrees, and which are energy dependent. Such distributions have been observed during magnetic storms (Horne et al. 2003a). Fourth, careful modeling of the observed wave power which takes account of both bounce averaging and MLT variations gives a timescale for electron acceleration of the order of 1–2 days, which is comparable with the observed timescale for acceleration (Horne et al. 2005b).

Until now acceleration by whistler mode waves, treated in quasi-linear diffusion theory, has been the most studied local acceleration process. However, other types of waves such as magnetosonic waves (Horne et al. 2007) and highly non-linear interactions with individual

chorus elements are also important in producing acceleration (Katoh and Omura 2007), and these processes require more research. Also, acceleration by lightning-generated whistler wave packets has been proposed as an important acceleration mechanism (1). This acceleration takes place when gyroresonant electrons are trapped by the wave field. The acceleration rate in this regime is much greater than that of stochastic acceleration in the untrapped regime. Further, other processes such as transit time damping may also be important (e.g., Summers and Ma 2000).

Electron Loss. As an electron drifts around the Earth it may encounter several different types of waves. Some waves, such as whistler mode chorus, contribute to acceleration while others, such as plasmaspheric hiss and electromagnetic ion cyclotron (EMIC) waves, contribute to electron loss to the atmosphere. In addition, outward radial diffusion onto open drift orbits as a result of changes in the outer magnetopause boundary may also contribute to electron loss.

Inside the plasmapause, which terminates the near-Earth plasmasphere filled with high-density cold plasma, there are three types of waves that can contribute to electron loss via scattering into the loss cone. These are plasmaspheric hiss, lightning generated whistlers, and whistler mode waves from ground based transmitters (Abel and Thorne 1998). Hiss tends to dominate the loss rates in the outer plasmasphere at energies from a few hundred keV to a few MeV (Meredith et al. 2006). Lightning becomes more important at lower L. The effect of transmitters tends to dominate at low L (typically less than $L = 2$).

In the region where the plasmasphere overlaps with the ring current, EMIC waves, at frequencies between the proton and the helium gyrofrequency and between the helium and the oxygen gyrofrequency, are, theoretically, very effective in scattering radiation belt electrons into the loss cone (Summers and Thorne 2003; Albert 2003; Glauert and Horne 2005). However, there is little observational evidence of the presence of these waves and more data is required in order to assess their importance on a global scale.

Outside the plasmapause, whistler mode chorus can also contribute to electron loss as well as to electron acceleration. Whether loss exceeds acceleration depends on several factors, but losses tend to dominate when the ratio of the electron plasma frequency to the electron cyclotron frequency is large. Thus, information on the plasma density during magnetic storms is very important for determining losses to the atmosphere. EMIC waves are also observed outside the plasmapause but there their influence is restricted to scattering electrons with higher energies, typically above 1 MeV, into the loss cone (Meredith et al. 2003b).

Global Modeling. For a long time a balance between inward radial transport and electron loss to the atmosphere has been recognized to be an important process governing the structure of the quiet time radiation belts (Lyons and Thorne 1973). Recently, several models have been used to study flux variations in the radiation belts where loss due to wave-particle interactions is treated as a simplified loss term. These models show that the flux at the heart of the radiation belts has, hitherto, been underestimated when satellite data at geostationary orbit are used as an outer boundary (Brautigam and Albert 2000; Shprits and Thorne 2004; Shprits et al. 2006b; Lam et al. 2007), and, thus, additional local wave acceleration processes must be incorporated into the radiation belt models.

One of the most comprehensive global models of the radiation belts is called Salammbô (Beutier and Boscher 1995; Bourdarie et al. 1997). It is based on a Fokker-Planck equation where originally radial transport (radial diffusion), Coulomb collisions, and losses due to plasmaspheric hiss were included as diffusion processes. Wave acceleration and losses due

to whistler mode chorus waves have now been incorporated in Salammbô, using diffusion coefficients from the PADIE code (Glauert and Horne 2005) together with a database of whistler mode chorus waves (Meredith et al. 2001, 2003c), showing that wave acceleration provides a viable process to increase the flux on a global scale during magnetic storms (Varotsou et al. 2005, 2008). Salammbô has also been used to model the radiation belts when a co-rotating interaction region (CIR) between a fast and a slow solar wind stream interacts with the Earth's magnetosphere, and the model shows that wave acceleration can result in a major increase in the radiation belt electron flux during weak long-duration magnetic storms (Horne et al. 2006). A number of new pitch angle diffusion studies (e.g., Albert 2005; Ni et al. 2008) and new global radiation belt models have been developed (e.g., Miyoshi et al. 2006; Fok et al. 2008; Varotsou et al. 2008), which show that electron acceleration by whistler mode chorus waves is a key physical process that must be included for storm time simulation of the radiation belts.

Effects of Radiation-Belt Electrons on the Ionosphere. A variety of physical processes occurring in the ionospheric plasma is driven by the fluxes of energetic particles or electromagnetic waves generated in the region of the radiation belts. The electromagnetic energy originating in lightning discharges escapes into the magnetosphere and propagates as a whistler mode wave, which pitch-angle scatters (and thus precipitates) energetic electrons, thereby generating hard X-rays through bremsstrahlung (Feldman et al. 1996; Bucik et al. 2006). Furthermore, precipitating electrons cause localized ionization and changes of ionospheric plasma conductivity (Demirkol et al. 1999). The feedback of magnetospheric Alfvén waves and varying ionosphere conductivity lead to the creation of complex magnetosphere–ionosphere current systems (e.g., Pokhotelov et al. 2004). Moreover, scattering of relativistic electrons by EMIC waves can also drive the X-ray bursts in the ionosphere (Lorentzen et al. 2000; Millan et al. 2002, 2007). Future investigations of the simultaneous registration in the topside ionosphere of X-rays and HF waves within the time frame of the ASIM (Atmosphere-Space Interactions Monitor) project on board the International Space Station as well as on board the low orbiting TARANIS (Tool for the Analysis of RAdiations from lightNIngs and Sprites) satellite could bring new information concerning this process and its impact on the upper atmosphere.

HF diagnostics located on a low orbiting satellite in the topside ionosphere detected an intensity increase of about 20 dB above the background, located in particular over the Euro-Asia region (Klos et al. 1997). These remarkable HF emissions were correlated with the positions of the maximum fluxes of precipitating particles in the outer radiation belts, as determined by high-energy particle measurements in the 0.5–1.5 MeV energy range. Permanent pumping of electromagnetic waves from the ground to the ionosphere and the precipitation of energetic particles from the radiation belts can, thus, disturb the top-side ionosphere and lead to enhanced turbulence in the ionospheric plasma. The scattering of supra-thermal electrons of radiation belt origin on ion-acoustic or Langmuir turbulence was proposed as a mechanism for the generation of broad-band HF emissions (Rothkaehl and Klos 2003; Rothkaehl and Parrot 2005).

Recent monitoring of the space plasma environment has shown that electromagnetic noise detected at ionospheric altitudes can be generated due to cataclysmic processes occurring on the surface of the Earth (Pulinets 2007). A case study of HF-wave and gamma-ray measurements performed on-board the CORONAS-I satellite showed simultaneous enhancements in whistler wave activity and in soft gamma-ray fluxes over a seismic center. Precipitating energetic electrons stimulate the excitation of HF whistler mode emission via the incoherent Čerenkov mechanism. The proposed process has a cascade-like character (Rothkaehl and Parrot 2006).

4 Engineering Models for the Radiation Environment

In this section, we describe models that are commonly used in satellite engineering applications as well as some science models that are presently being developed for the same purpose.

4.1 SEP Flux and Fluence Models

For the purposes of implementing satellite/spacecraft design and estimating astronaut exposure to radiation, several SEP models were developed based on historical records of SEP events. Modisette et al. (1965), for example, elaborated a FORTRAN code using SEP events (with energies >30 MeV and >100 MeV) identified during the maximum phase of solar activity cycle 19 (1956–1961). Probability distributions were obtained for the total proton flux during missions ranging from 1 to 104 weeks. Later on, King (1974) derived a model to predict mission integrated SEP fluences using a database covering 1966–1972. The code version of this model is called SOLPRO (Stassinopoulos 1975) and it offers outputs at energies from >10 MeV to >100 MeV. Both models, however, depend on the original database because "ordinary" and "anomalously large" SEP events seem to behave as two different particle populations. Using data from cycles 19–21 this limitation was overcome by the JPL-85 model (Feynman et al. 1990). It works only for seven active years (i.e., outside solar minimum time periods). The JPL model uses a log-normal distribution to fit the solar proton event size distribution. The version JPL-91 (based on data from 1963 to early 1991) is run after selecting a lower threshold value to start proton fluence computation in various integrated energy channels (from >1 MeV to >60 MeV; Feynman et al. 1993). More details are given by Feynman et al. (2002).

A prediction attempt based on the log-normal approach was also performed by Escudier et al. (2002); the ONERA solar proton model employed IMP/GOES SEP measurements from 1974 to 2002 with energies up to 300 MeV. The SEP fluences derived from the model are differential and they were intended for any mission duration, even during the solar minimum phase (Boscher et al. 2003). No progress with regard to this work has been reported recently (D. Boscher, private communication, 2008).

The ESP (Emission of Solar Protons) model predicts integral omnidirectional solar proton fluences at 1 AU, at energies from >1 MeV to >300 MeV (Xapsos et al. 1999a) during solar active years. The model employs satellite measurements for three complete solar cycles (20–22) with a truncated power-law distribution and the maximum entropy method (Xapsos et al. 1999b, 2000). It is able to predict cumulative solar proton fluences and worst-case solar proton events as functions of mission duration and user confidence level. Xapsos et al. (2004) improved this model (using IMP/GOES data) for proton fluence-energy spectra op to >327 MeV, and considering solar minimum and solar maximum time periods (PSYCHIC model). Xapsos et al. (2007) extended the PSYCHIC model to cumulative solar heavy ion energy-LET spectra for the solar maximum phase.

Figure 7 shows, moreover, that outstanding SEP events can occur outside active years. Storini et al. (2008a) in their Fig. 3 demonstrated that the strength of SEP parameters undergoes a depletion within the Gnevyshev Gap (Storini et al. 2003, and references therein). Indeed, the relationship between SEP parameters and sunspot variability was extensively investigated at Moscow State University (MSU) since the 1990s. In this regard Nymmik (1999a, 1999b) described a model to evaluate the SEP fluence distribution as a function of the level of solar activity based on the analysis of IMP data (recorded during solar cycles 20–22), combined with proton fluxes derived from the analysis of radionuclides in lunar rocks.

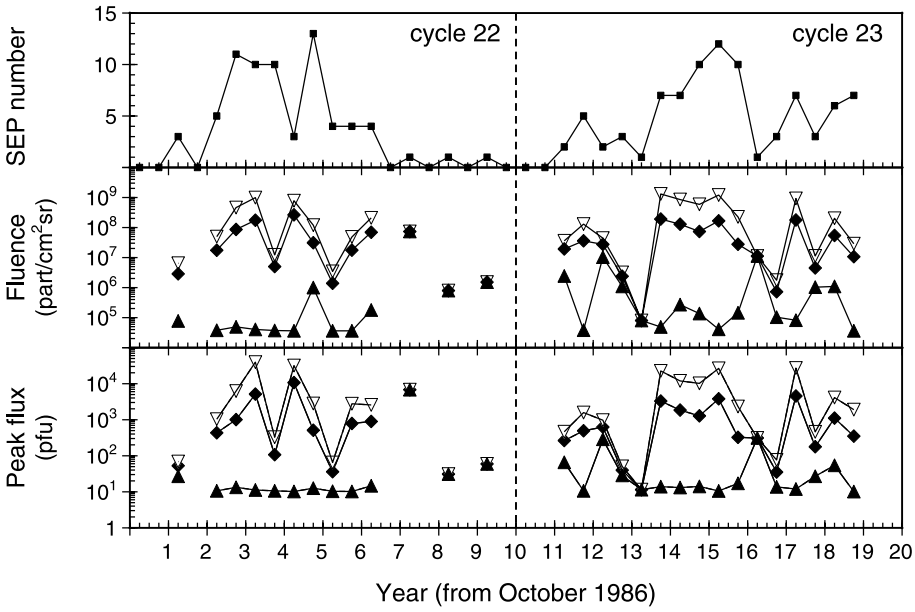

Fig. 7 The *upper panel* illustrates the number of solar proton events ($J[E > 10$ MeV$] > 10$ pfu) identified during each semester, from October 1986 to September 2005 by Laurenza et al. (2007). The *middle* and *bottom panels* show the maximum (*empty triangles*), mean (*diamonds*) and minimum (*filled triangles*) fluence and peak flux, respectively

In this model, the SEP fluence distribution follows a power-law function with an exponential steepening in the case of large fluences (see also Nymmik 2001). This model applies to solar proton fluences in the range 10^6–10^{11} protons cm^{-2} for proton energies >30 MeV and it was used to infer the yearly minimum and maximum SEP event number expected during solar cycle 24 (Storini et al. 2008a). This, so-called, MSU model (Nymmik 1999c) is able to compute, for a given probability level, the ≥10 MeV/nucleon SEP fluences and peak fluxes in near-Earth space for protons and heavier ions up to nickel. Details concerning a recent version of the model are given by Kuznetsov et al. (2005) and Nymmik (2008).

A new code for modeling the interplanetary solar high-energy particle environment was presented by Jun et al. (2007a). This model uses data from IMP-8 (from 1973, day 305, to 1997, day 319) obtained during the active part of the solar cycle combined with a virtual data set, to generate a smooth distribution of SEP fluences for interplanetary missions of any duration. The basis of the model (intended as a new JPL interplanetary solar proton model) comes from the preliminary Solar Probe Mission Study, which was performed by flying a virtual spacecraft through the database with an appropriate radial dependence of the flux being applied at each time step. (See Jun et al. 2007b, for more details.)

SOLPENCO (Solar Particle Engineering Code) is an operative code developed at the University of Barcelona to predict proton flux and fluence profiles of SEP events associated with interplanetary shocks (Aran et al. 2006). The code provides these profiles (from the onset of the event up to the arrival of the associated CME-driven shock) at 0.125, 0.250, 0.5, 1, 2, 4, 8, 16, 32 and 64 MeV for observers located at either 1.0 AU or 0.4 AU. SOLPENCO also furnishes the transit time and velocity of the shock from the Sun to the observer. Examples of the validation of the model using some case studies are discussed by Aran et al.

(2005a, 2005b). The background physics is described by Sanahuja et al. (2008). (See also Waterman et al. 2009.)

The available engineering models for estimating SEP fluxes and fluences are summarized in Table 1.

4.2 SEP Event Forecasting

Available physical SEP models are not able to predict the main characteristic parameters of each SEP event (e.g., SEP event start time, peak flux, fluence and the corresponding energy spectrum). This is due to the complexity of physical processes involved in the generation/acceleration and transport of SEPs in space (see Sect. 3.2). On the other hand, a forecasting technique for SEP event occurrence in the near-Earth environment needs to fulfill at least the following constraints: (i) accuracy (minimizing the number of lost events), (ii) reliability (avoiding false alarms), (iii) prompt warning (or fast alarm) and (iv) automation (codes running on informatics systems). To our knowledge, only semi-empirical models, based on observed SEP events and some other experimental/theoretical results, are presently available. (See Laurenza et al. 2009, for more details.) Two of these models, called PROTONS and PROTON PREDICTION SYSTEM (PPS), were extensively tested against observations of SEP events recorded at 1 AU and independently validated in terms of their probability of detection (PoD) and false alarm rate (FAR). These models are run after the occurrence of a solar flare and use the observed flare parameters as inputs to the forecasting algorithm.

The PROTONS code, taken in real-time operation during the 1970s (Heckman 1979; Balch and Kunches 1986; Heckman et al. 1992), is based on precursor information statistically related to SEP event occurrence (X-ray flare location, X-ray half-power fluence and Type II/IV radio burst occurrence). The PROTONS code (see Balch 1999, for details) is presently running at NOAA/SWPC (see http://www.swpc.noaa.gov/alerts/archive.html for alerts issued from 1997 to present). The main outputs of the code are SEP event occurrence probability, predicted SEP rise time (time from X-ray flare maximum to SEP flux maximum), and the predicted peak flux at Earth.

The PPS code, initially called PPS76, was introduced by Smart and Shea (1979) and updated to PPS-87 (Advanced Proton Prediction System; Smart and Shea 1989) at the AFRL/Hascom. Its input parameters are: flare signatures, fixed time for particle injection into the interplanetary magnetic field (0.25 h after flare onset) and a longitudinal SEP intensity gradient. Outputs include: an SEP event occurrence flag (not a probability), timing, intensity, spectrum and elemental composition for different energy channels ($E_{\min} > 5$ MeV).

Neural network techniques are used at the University of Southampton for SEP forecasts (Gabriel and Patrick 2003); the ratio of GOES X-ray (hard and soft channels) fluxes is introduced as input (the best obtained success-rate was $\sim$65%). However, a high number of predicted SEP events was not actually observed (Gabriel 2008). Nevertheless, artificial neural networks are potentially useful tools to improve SEP event forecasts; currently they are also used in near-real time for some other applied SEP models (e.g., SEP event dose-time profiles, Hoff and Townsend 2003). Such applied SEP models evaluate the impact of charged-particle fluxes on materials, instruments and biological bodies. (See, e.g., Tylka et al. 1997, for CR effects on micro-electronics.)

The empirical relation between SEP occurrence and X-ray flare characteristics has been exploited by other researchers. Among these characteristics (and the respective studies) we recall: the hard X-ray spectral evolution in solar flares (Garcia 1994a; Kiplinger 1995), the temperature of soft X-ray flares (Garcia 1994b) and the integrated solar X-ray flux (Kubo and Akioka 2004). In particular, forecasting methods for the occurrence of an SEP event and its magnitude were discussed by Garcia (2004a, 2004b).

Table 1 Overview of engineering models of SEP flux and fluence

Model	Input	Output	Operat.	Implement.	Availability and/or Reference
KING/SOLPRO	Mission duration, energy threshold, confidence level	Mission integrated proton fluence	Yes	Fortran	ftp://hanna.ccmc.gsfc.nasa.gov/pub/modelweb/solar/proton_flux/solpro/; King (1974), Stassinopoulos (1975)
JPL Proton Fluence	Mission duration during the active years, confidence level	Fluence of protons with energy >10 and >30 MeV	Yes	Fortran	http://modelweb.gsfc.nasa.gov/sun/jpl.html; Feynman et al. (1993, 2002)
JPL-Solar Probe	Mission duration, confidence level	Mission-integrated fluence and peak flux for protons and heavier ions	Intended		Jun et al. (2007a)
ESP	Mission duration, confidence level	Probability of cumulative or exceeding fluence (worst case event distribution) vs. >30 MeV fluence	Yes		http://www.spenvis.oma.be/ Xapsos et al. (1999a, 1999b, 2000)
PSYCHIC	Mission duration, confidence level	ESP extension to solar minimum	Intended		Xapsos et al. (2004, 2007)
SEP model 2004 (MSU updated)	Time period, probability	fluence and peak flux of protons with energy $4 \div 10^4$ MeV	Yes		http://srd.sinp.msu.ru/nymmik/models/sep.php
SOLPENCO	Heliolongitude of the flare/CME, heliocentric distance, shock transit time, shock width, mean free path, turbulence foreshock region (yes/no)	Profile of proton fluxes and anisotropy at the observer location for 6 energy levels between 0.25 and 8 MeV	Yes	IDL	http://www.am.ub.es/~blai/enginmodel/SEP_Abstract.html#ref7

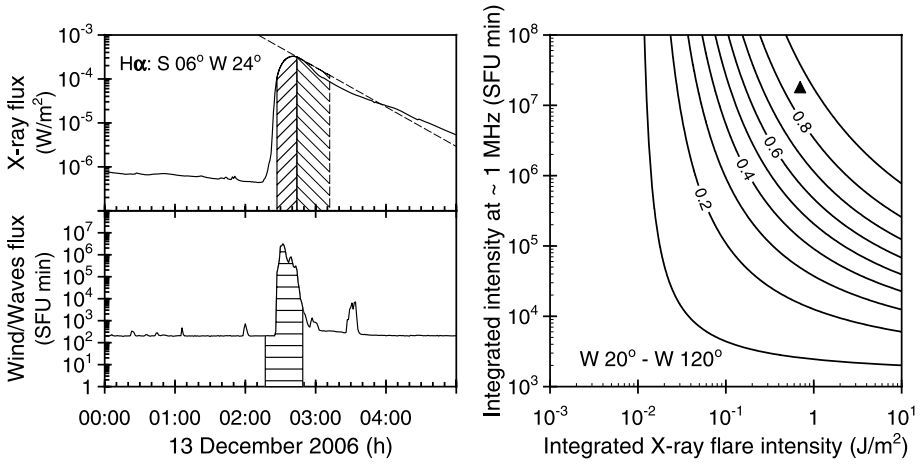

Fig. 8 Probability contours for the occurrence of an SEP event as a function of the integrated X-ray and radio intensity for the reported heliographic longitudinal interval (*right panel*); the marker refers to the 13 December 2006 SEP event. The soft X-ray flux time history (*solid line*) derived from GOES 11 measurements is reported in the *left upper panel*; the *dashed line* represents the slope of the extrapolated exponential fit used for the fluence evaluation: the *left hatched area* indicates the fluence based on the actual data (computed from the 1/3 power point before the peak flux to 6 min later) and the *right hatched area* gives the fluence based on the extrapolation procedure (computed from 6 min after the peak to the 1/3 power point during the decay phase). The *left bottom panel* shows the 1 MHz radio flux from WIND (with integration indicated by horizontal hatching from 10 min before to 10 min after the soft X-ray peak flux)

Laurenza et al. (2009) developed a forecasting tool that gives the probability of the occurrence of an SEP event (with *Event Start* defined as the time when the proton flux J [>10 MeV] ≥ 10 cm^{-2} s^{-1} sr^{-1} for three consecutive 5-min intervals; and *Event End* defined as the time when J falls below the above threshold) after an $\geq$ M2 X-ray flare, within 10 minutes of the flare peak time (see, for preliminary results, Laurenza et al. 2007; Storini et al. 2008c). This model, which is based on the logistic regression analysis of a database covering eleven years (1995–2005) of GOES/WIND data, shows the capability to distinguish between proton associated flares and flares that are not associated with proton events by using: (i) the time integrated flux of the soft X-ray flare (as a quantitative measure of both the flare importance and its duration), (ii) the flare longitude and (iii) the integrated intensity of the type III radio emission (related to the solar particle acceleration/escape from the Sun). Figure 8 (right panel) exemplifies the probability levels computed for the heliographic longitude interval of W20°–W120°, together with the time integrated X-ray intensity and radio emission at $\sim$1 MHz estimated for an SEP event on 13 December 2006 (note that this event is outside the period covered by the SEP catalog used to generate the model). It can be seen that the corresponding marker (filled triangle) lies above the 80% probability level. The left panel of Fig. 8 illustrates the method of deriving the integrated parameters needed for the SEP forecast. The evaluation over the 93 SEP events identified from 1995 to 2005 yielded a PoD $= 63\%$ and a FAR $= 42\%$ for the prediction model.

An up to 1-hour forecast technique for solar proton events, by using relativistic electron intensities in space (since electron onset precedes proton onset), was introduced by Posner (2007). This method was tested using SOHO/COSTEP data recorded over eleven months of 2003. Also, a detailed description of a possible advanced forecast method was furnished, including the forecasting contingency matrix and the evaluation of false and missed warnings

(see Table 3 of Posner 2007). The model in its present version is only able to forecast SEP event onsets, but it looks to constitute a promising forecasting technique. Also, the use of real-time records of GLEs from the world-wide network of ground-based CR detectors has been proposed to provide earliest alerts for SEP onsets, and these codes are now undergoing testing/implementation (e.g. Dorman et al. 2003; Kuwabara et al. 2006; Mavromichalaki et al. 2007).

4.3 SEP Catalogs/Lists

Although they are no real models of SEP event occurrence or of SEP fluxes, SEP event catalogs constitute an important resource in studies of SEPs. There exist several catalogs/lists of SEP events for past times (see McDonald 1963, for early work). These are available as data books, lists in published papers and on-line SEP lists. Table 2 presents a selection of them, organized as follows: books (top panel), published papers (middle panel) and websites (bottom panel).

Data books (see top panel of Table 2) are very useful because, besides the event characteristic parameters (year, month, day, onset and peak time), they report the importance of the SEP event, information on the spacecraft and the energy channels used or the type of ground based observations employed (balloon flights, NMs, riometer measurements). They fully describe an SEP event by also reporting the energy spectra and time profiles of proton fluxes in several energy bands. Moreover, these data books contain parameters of the solar activity that can be associated with each SEP event. Sometimes for the association with a solar source a confidence degree is also provided (certain, probable, possible, contributing).

In general, the solar source associated with an SEP event is identified by the active region number and the coordinates of the flare on the solar disk. Then, many observational data accompanying the source activity are given with their temporal evolution (onset, maximum, end): H_α flares, soft X-rays, hard X-ray bursts in different energy ranges, solar radio emissions at fixed frequencies and the dynamic spectra of metric bursts.

Lists given in published papers (see middle panel of Table 2) or on-line SEP lists (see bottom panel of Table 2) do not present a similarly complete description of the SEP events, but rather furnish basic information about the time and size both of the SEP event and of the H_α and/or X-ray associated flare.

Nevertheless, it should be remarked that:

- when a list provides also the association to a solar source the so-called Big Flare Syndrome approach (i.e., selection of the largest flare near the particle onset; Kahler 1982) was used. In some cases the identification of the parent flare was doubtful and subjective, especially when data on individual CMEs were not used to fully characterize each event. This introduces some uncertainties in the reliability of the SEP lists.
- the lists show some inconsistencies relative to each other. This is mainly due to the different criteria adopted in defining an SEP event (the current most widely used definition of a proton event is the NOAA one, where a threshold of 10 pfu [1 pfu = cm^{-2} s^{-1} sr^{-1}] for proton fluxes is assumed at energies >10 MeV, measured onboard GOES satellites). In fact, these catalogs may differ in (i) the selection of the proton flux threshold for the definition of the commencement of an SEP event, (ii) the particle energy channels used from the same instrument or from different instruments; and (iii) the data bases employed, which often cover different time intervals.

Table 2 SEP catalogs/lists. Acronyms I.E. [N.I.E.] mark the sources that do [do not] resolve all individual events; V.D. indicates the use of velocity dispersion

Reference	Period	Energy [MeV]	Minimum flux	Comment
Svestka and Simon (1975)	1955–1969	>10	0.1 pfu (before Dec. 1965)	N.I.E.
			0.01 pfu (Dec 1965–Dec 1969)	N.I.E.
Akiniyan et al. (1983)	1970–1979	>10	1 pfu	I.E.*
Bazilevskaya et al. (1990)	1980–1986	>10	1 pfu	I.E.*
Sladkova et al. (1998)	1987–1996	>10	1 pfu	I.E.*
Van Hollebeke (1974, 1975)	May 1967–Dec 1972	>20–80	10^{-4} pfu MeV^{-1}	N.I.E.
Nonnast et al. (1982)	Nov 1973–Sep 1977	2–4.60		V.D.
Cliver et al. (1989)	Feb 1980–Jan 1985	20–40	10^{-3} pfu MeV^{-1}	V.D.; I.E.**
Shea and Smart 1990	1955–1986	>10	10 pfu	I.E.
Cliver and Cane 1990	1976–1986	>10	10 pfu	I.E.
Gentile et al. 1993	Jan 1987–Sep 1991	>10	10 pfu	I.E.
Gopalswamy 2003	1997–2001	>10	10 pfu	N.E.
Kurt et al. 2004	1970–2002	>10	10 pfu	I.E.
Cane et al. 2006	1997–2005	>10	10 pfu	I.E.
Jun et al. 2007a	May 1977–May 1984; May 1987–May 1994	>11.1	1 pfu (daily)	N.I.E.***
Laurenza et al. 2009	1996–2005	>10	10 pfu	I.E.
http://cdaw.gsfc.nasa.gov/LWS/data/event_list.html	1997–2001	>10	10 pfu	N.I.E.
http://www.swpc.noaa.gov/ftpdir/indices/SPE.txt	Jan 1976–Jul 2007	>10	10 pfu	N.I.E.
http://www.wdcb.rssi.ru/stp/data/PRCATFINAL/	1970–1996	>10	>1 pfu	I.E.*

*If the sources of the different proton enhancements were identified successfully

**The presence of ≥200 keV electrons is also required; threshold for I.E.: 5×10^{-3} pfu MeV^{-1}. Otherwise the complex particle flux increase was listed as one event

***Event flux threshold is 1 pfu averaged over each day; the end of an event is when the daily-averaged proton flux falls below the threshold

– the start and the end of a proton event is often defined in such a fashion that some lists allow multiple SEP events and/or interplanetary shock proton increases to occur during a single proton event; in other words, some lists do not resolve all the individual proton events.

4.4 GCR Flux and Fluence Models

Reliable models of the ion fluxes in GCRs are vital for the determination of LET spectra and resulting SEEs. The flux models must account for temporal variations in the ion fluxes due to solar modulation and also must cover the full species range from protons to very heavy ions.

A large volume of spectrum data obtained by satellite borne instruments, balloon experiments and NMs is now available, and is continuously expanded in the course of long-duration missions such as ACE. As a result, the CR environment is now well understood, and mature models have been developed.

In this section, only models of the GCRs will be considered, as these particles are the most harmful and models of their populations are much more advanced than models of the anomalous cosmic ray (ACR) component.

The first truly "operational" model of GCR fluxes was that implemented in CREME86, a suite of software tools developed for the estimation of single event upsets (SEUs) in microelectronics (Adams et al. 1981). The flux models were based on analytical function fits involving a limited number of ion species, with scaling factors for other ions. Flux variations due to the solar activity cycle were represented by a simple sine curve. CREME86 was later superseded by CREME96 (Tylka et al. 1997), which uses the GCR model developed by SINP/MSU (Nymmik et al. 1996). The Nymmik model is based on a more extensive data set, and models the solar cycle dependence as a function of sunspot number. This model has obtained the status of an ISO standard (15390). However, no official release of the model code is available, although several groups have coded applications using the ISO standard description document. A version of the Nymmik model can be run on the CREME96 web site (https://creme96.nrl.navy.mil/), but it is not clear which version of the model has been implemented. In addition, the CREME96 software is not available outside of the U.S. due to an ITAR restriction. The CREME86 model is available from its authors, and can be run on SPENVIS (http://www.spenvis.oma.be/).

Other models have, in addition, been developed, notably the CHIME model (Chenette et al. 1994) which is based on CRRES data, and the Badhwar-O'Neill model (O'Neill 2007) which makes extensive use of ACE data. Table 3 lists the available GCR models with their main characteristics.

Finally, we note that the model of Usoskin et al. (2005) can also be used for engineering purposes, if it is appended with appropriate LIS for the heavy elements.

4.5 Magnetospheric Transmission

Different possibilities are available today for computing cutoff rigidity and asymptotic direction for space weather purposes. Some groups have made their source code available (see Table 4). A world grid of vertical R_C on Earth and at low Earth orbit can be found in the literature (Smart et al. 2008a, 2008b). Recently, different web sites have been developed to offer the possibility to compute on-line the cutoff rigidity as a function of position, time and magnetic activity (see Table 4).

Table 3 Overview of currently available GCR models

Model	Energy range	Ions	Variability	Source	Reference
Nymmik	10–100,000 MeV	$1 \leq Z \leq 92$	Solar cycle phase (R_i)	ISO Standard 15390: http://www.iso.org/iso/iso_catalogue/catalogue_tc/catalogue_detail.htm?csnumber=37095	Nymmik et al. (1996)
Badhwar-O'Neill '07	1–10^6 MeV/nuc	$1 \leq Z \leq 28$	Solar modulation	http://www4.jsc.nasa.gov/org/Ev/ev5/index.html	O'Neill (2007)
CHIME	10–60,000 MeV/nuc	$1 \leq Z \leq 92$	Solar cycle modulation	http://www.kirtland.af.mil/library/factsheets/factsheet.asp?id=7899	Chenette et al. (1994)
CREME86	$\geq$ 10 MeV/nuc	$1 \leq Z \leq 92$	Solar cycle modulation (sine curve)	Available from the authors; implemented in SPENVIS	Adams et al. (1981)

Table 4 Magnetospheric CR transmission codes and models

Name/Reference	Output	*B* field models	Source	Run on-line at
Shea and Smart code	Cutoff rigidity	Tsyganenko (1989)	ftp://nssdcftp.gsfc.nasa.gov/models/cosmic_rays/cutoff_rigidity_sw/	no
MAGNETOCOSMICS	Cutoff rigidity Asymptotic direction Trajectory visualization	Tsyganenko (1989) Tsyganenko (1996) Tsyganenko and Sitnov (2005)	http://cosray.unibe.ch/~laurent/magnetocosmics	http://www.spaceweather.eu
Kudela and Storini code	Cutoff rigidity	(Tsyganenko (1989) with optional Dst extension) Tsyganenko and Sitnov (2005)	not available	http://www.spaceweather.eu
Bütikofer et al. (2008a)	Cutoff rigidity above the atmosphere interpolated from pre-computed grid	Tsyganenko (1989)	see MAGNETOCOSMICS source	http://cosray.unibe.ch
R_C vs. L	Cutoff rigidity dependence on the L shell parameter	Tsyganenko (1989)	Shea et al. (1987) Storini et al. (2008b)	
Nymmik et al. (2008)	parametrization of precomputed cut-off rigidity grid	Tsyganenko (1989)	published in (Nymmik et al. 2008)	

For a rapid first order estimate of the cutoff rigidity analytical approximations exist. By approximating the geomagnetic field by a dipole, the cutoff rigidity is expressed by the Störmer cutoff formula

$$R_{\mathrm{C}} = \frac{M \cos^4 \lambda}{r^2[1 + (1 - \cos^3 \lambda \cos \epsilon \sin \eta)^{1/2}]^2} \tag{6}$$

where M is the dipole moment, r is the distance from the dipole center, λ is the geomagnetic latitude, ϵ is the azimuthal angle measured clockwise from the geomagnetic east direction (for positive particles), and η is the angle from the local magnetic zenith direction (Cooke et al. 1991). Shea et al. (1987) have shown that the vertical effective cutoff rigidity $R_{\mathrm{C}}^{\perp}$ and the McIlwain L shell parameter are linked approximately by the relation

$$R_{\mathrm{C}}^{\perp}[\mathrm{GV}] = K L[R_{\mathrm{E}}]^{-\alpha} \tag{7}$$

where K and α depend on the epoch considered. Recently Storini et al. (2008b) extended this study and found that the equation with $K = 16.293$ and $\alpha = 2.073$ provides the best fit to compute cutoff rigidity at low and mid latitudes for the period 1955–1995. Bobik et al. (2006) published a geomagnetic transmission function for the orbit of the shuttle flight carrying the AMS-01 magnetic spectrometer experiment. Recently, different magnetospheric transmission models based on the interpolation or parametrization of a precomputed cutoff rigidity grid have also been developed (Bütikofer et al. 2008a; Smart et al. 2006; Nymmik et al. 2008).

4.6 Radiation Belt Models

This section is devoted (and limited) to a class of models known as 'semi-empirical'. In general, this type of model consists of a set of particle flux look-up tables and interpolation and/or extrapolation routines. The look-up tables are of the form $J(E, P, t, \nu)$, where J is the particle flux or fluence for a given species, E is the particle energy, P represents a position in space, t is an epoch, and ν represents one or more additional parameters that characterize, for instance, the state of the magnetosphere (defined as a state vector by Fung et al. 2005).

P is usually expressed in terms of McIlwain's (B, L) coordinates (McIlwain 1961) or derivatives thereof. However, geographic coordinates are sometimes used as well, and in at least one case there is no position input (the POLE/IGE model Sicard-Piet et al. (2006, 2008), for example, is valid for the geostationary environment). When the epoch t is present, it usually refers to a phase in the solar cycle. Finally, the state vector ν is used to accommodate additional, driving, parameters such as magnetic or solar wind indices to represent the state of the magnetosphere (quiet, moderately or highly perturbed, ...).

The first suite of semi-empirical models was developed by NASA in the 1960's and early 70's, culminating in the venerable model sets AP-8 (Sawyer and Vette 1976) and AE-8 (Vette 1991), for protons and electrons, respectively. Based on data sets from a number of satellite missions, these models cover the whole spatial region of the radiation belts and most of the energy range of importance for radiation effects. Newcomers in the field of radiation belts will be amazed to discover that these decades old models are still the de facto standards for engineering purposes, although to all intents and purposes they are badly outdated. Their lasting success is due to the complexity of the radiation belt environment and the difficulties inherent in modeling its populations properly. Several models have been developed since the emergence of AP-8 and AE-8 (see Tables 5 and 6), but none of them combines coverage

Table 5 Overview of currently available empirical trapped proton models

Model	Energy range	Coordinate range	Magnetic field models	Variability	Source	Reference
AP-8 MIN	0.1–400 MeV	$1.14 \leq L \leq 6.6$ $1.0 \leq B/B_0 \leq$ loss cone	Int.: Jensen & Cain (Jensen and Cain 1962) Ext.: None	Fixed	http://modelweb.gsfc.nasa.gov/magnetos/aeap.html	Sawyer and Vette (1976)
AP-8 MAX	0.1–400 MeV	$1.14 \leq L \leq 6.6$ $1.0 \leq B/B_0 \leq$ loss cone	Int.: GSFC 12/66 (Cain et al. 1967), updated to 1970 Ext.: None	Fixed	http://modelweb.gsfc.nasa.gov/magnetos/aeap.html	Sawyer and Vette (1976)
CRRESPRO	1.1–90.0 MeV	$1.0 \leq L \leq 5.5$ $1.0 \leq B/B_0 \leq 684.6$	Int.: IGRF 1990 Ext.: Olson-Pfitzer quiet (Olson and Pfitzer 1974)	Solar max., quiet/active	http://www.kirtland.af.mil/library/factsheets/factsheet.asp?id=7899	Meffert and Gussenhoven (1994)
PSB97	18–500 MeV	$1.1 \leq L \leq 2.0$ $90° \geq \alpha_0 \geq$ loss cone	Int.: IGRF 1995 Ext.: None	Solar min.	Available from the author (Fortran code + model maps)	Heynderickx et al. (1999)
LATRM	$>$ 16, 30, 80 MeV	250–850 km	Int.: IGRF Ext: None	$F_{10.7}$ dependence, secular variation	http://see.msfc.nasa.gov/ire/model_low_altitude.htm	Huston and Pfitzer (1998)
TPM1	1.5–81.5 MeV	300 km $\leq$ GEO $1.0 \leq B/B_0 \leq$ loss cone	Int.: IGRF Ext: Olson-Pfitzer quiet (Olson and Pfitzer 1974)	$F_{10.7}$ dependence, secular variation, nominal quiet and active	http://see.msfc.nasa.gov/ire/model_tpm.htm	Huston (2002)

Table 6 Overview of currently available empirical trapped electron models

Model	Energy range	Coordinate range	Magnetic field models	Variability	Source	Reference
AE-8 MIN	0.04–7 MeV	$1.14 \leq L \leq 12$ $1.0 \leq B/B_0 \leq$ loss cone	Int.: Jensen & Cain (Jensen and Cain 1962) Ext.: None	Fixed	http://modelweb.gsfc.nasa.gov/magnetos/aeap.html	Vette (1991)
AE-8 MAX	0.04–7 MeV	$1.14 \leq L \leq 12$ $1.0 \leq B/B_0 \leq$ loss cone	Int.: Jensen & Cain (Jensen and Cain 1962) Ext.: None	Fixed	http://modelweb.gsfc.nasa.gov/magnetos/aeap.html	Vette (1991)
CRRESELE	0.5–6.6 MeV	$2.5 \leq L \leq 6.8$ $1.0 \leq B/B_0 \leq 684.6$	Int.: IGRF 1990 Ext.: Olson-Pfitzer quiet (Olson and Pfitzer 1974)	A_{p15} dependence	http://www.kirtland.af.mil/library/factsheets/factsheet.asp?id=7899	Brautigam and Bell (1995)
POLE/IGE	0.001–5.2 MeV	GEO	None	mission start year, mission duration	Available from the authors	Sicard-Piet et al. (2006, 2008)
FLUMIC	0.2–5.9 MeV	$3.0 \leq L \leq 8.0$	Int.: IGRF 1994 Ext.: Tsyganenko (1989)	Solar cycle	Available from the authors	Rodgers et al. (2004)
ESA-SEE1	0.04–7 MeV	$1.14 \leq L \leq 12$ $1.0 \leq B/B_0 \leq$ loss cone	Int.: Jensen & Cain (Jensen and Cain 1962) Ext.: None	Fixed	http://ccmc.gsfc.nasa.gov/modelweb/magnetos/radmodls.html	Vampola (1996)

in space and energy like the NASA models. Barth et al. (2003) and Lauenstein and Barth (2005) present an extensive historical review and comparison of most of the current radiation belt models.

In 1996, a COSPAR panel was created to coordinate international efforts to create a new generation of radiation belt models. The panel was originally called *Panel on Standard Radiation Belts (PSRB)* but was renamed *Panel for Radiation Belt Environment Modeling (PRBEM)* in 2004 (http://craterre.onecert.fr/prbem/). Recently, the Next Generation Radiation Specifications Consortium (NGRSC) was formed as an informal group of researchers pursuing various methods to replace the existing models (O'Brien 2006). The principal participants in the NGRSC are from The Aerospace Corporation, Los Alamos National Lab, Air Force Research Lab, and ONERA.

The PRBEM and NGRSC groups came to the conclusion that the usage of data assimilation tools is necessary for the development of accurate dynamic radiation belt models. Data assimilation will allow to intercalibrate various measurements and combine them with a physics based model. Such blending of past observations and models is usually referred to as reanalysis. Through reanalysis, the evolution of the radiation belt fluxes can be studied with high resolution in time and space, at the same time minimizing observational errors. For more details see, for example, Kondrashov et al. (2007), Shprits et al. (2007), and Koller et al. (2007).

4.7 Atmospheric Effects and Dose Models

Different Monte Carlo packages such as Geant4 (Allison et al. 2006), FLUKA (Fasso et al. 2005), and MNCPX are available for modeling the interaction of particles with user defined complex geometry. These codes differ in several aspects, as for example the type of physical models used, the way of defining the geometry, and the informatics language in which they are written. Different authors have used these Monte Carlo packages or their own codes (Monte Carlo and deterministic) to model the interactions of CRs with the Earth's atmosphere. Two of these CR codes are publicly available: PLANETOCOSMICS and CORSIKA. The PLANETOCOSMICS code is a Geant4 application that computes the interaction of energetic particles (<1 TeV) with the Earth, Mars and Mercury (Desorgher et al. 2005; Bütikofer et al. 2008b). This takes into account the planetary atmosphere, magnetic field, and soil. The CORSIKA code is a program for detailed simulation of extensive air showers initiated by high energy CR particles (Heck 2006). The PLANETOCOSMICS and CORSIKA codes are open source and can be run on personal computers. The Qinetiq Atmospheric Radiation Model (QARM) is a web based application that can be used to compute secondary CR spectra in the atmosphere as a function of position and time as well as to compute effective dose for air crews (Lei et al. 2006).

Two models of the ionization of the Earth's atmosphere by CRs, which have been recently developed and made available to the scientific community, have potential for being developed for engineering purposes. Among these, the Oulu ionization model, based on CORSIKA, has been published in the form of yield functions while the Bern ionization models, based on PLANETOCOSMICS, can be used on-line (Usoskin and Kovaltsov 2006; Usoskin et al. 2009a).

Different codes are available to compute the radiation exposure on-board airplanes due to GCRs. These offer the possibility to compute the dose accumulated during user defined flights. The European EPCARD, SIEVERT and QARM dose models are operational on the web while the U.S. CARI code is provided as a DOS application.

Table 7 Atmospheric effect and dose models

Name	Output	Reference	Source	Run on-line at
CORSIKA	Extensive air shower parameters Secondary particle spectra deposited energy in atmosphere	Heck (2006)	http://www-ik.fzk.de/corsika/	
PLANETOCOSMICS	Secondary particle spectra in atmosphere Deposited energy in atmosphere Visualization	Desorgher et al. (2005) Bütikofer et al. (2008a)	http://cosray.unibe.ch/~laurent/planetocosmics	
QARM	Secondary particle spectra in atmosphere Radiation Dose for air crew	Lei et al. (2006)		http://geoshaft.space.qinetiq.com/qarm/
EPCARD	Radiation Dose for air crew			http://www.helmholtz-muenchen.de/epcard2/index_en.phtml
SIEVERT	Radiation Dose for air crew			http://www.sievert-system.org/WebMasters/fr/partenaires.html
CARI6	Radiation Dose for air crew		http://www.faa.gov/education_research/research/med_humanfacs/aeromedical/radiobiology/cari6/download/	
Oulu CRAC model	Earth's atmosphere Ionization by GCRs Computed with CORSIKA/FLUKA	Usoskin and Kovaltsov (2006), Usoskin et al. (2009a)	Yield functions and description in Usoskin and Kovaltsov (2006), Usoskin et al. (2009a)	
Bern ionization model	Earth's atmosphere Ionization by GCRs Computed with PLANETOCOSMICS	Bütikofer et al. (2008b)		http://cosray.unibe.ch/~laurent/atmosphere_ionisation_by_cosmic_rays/

5 Outstanding Issues

5.1 Scientific Challenges

GCR Modulation. One of the main physical challenges in modeling GRC modulation is that of providing a reliable description of the diffusion tensor throughout the heliosphere. This task is extremely difficult since it is affected by several unsolved questions of heliospheric research: What is the nature of turbulence in the heliospheric plasma and how does it affect particle transport parallel and perpendicular to the mean magnetic field? What is the form of the mean magnetic field throughout the heliosphere? What is the role of drifts and how are they affected by turbulence? What is the correct description of the effect of individual large CMEs/CIRs on cosmic-ray modulation, and how do they affect fluxes on short time scales (Forbush decreases)? Unfortunately, many of these problems are very difficult to address without a large set of in-situ measurements from large distances (up to several hundred AU) and good heliolatitudinal and longitudinal coverage. Thus, for the foreseeable future, we will be forced to use semi-empirical relations such as the force-field model to quantitatively describe the spectrum of cosmic rays in near-Earth space. Fortunately, the good correlation between solar activity indices (e.g., the sunspot number) and the modulation potential makes it possible to forecast, rather reliably, the cosmic-ray environment on solar-cycle time scales.

SEP Acceleration and Transport. One of the main issues of SEP acceleration at the Sun involves the relative role of flares and CMEs in the acceleration process. In order to achieve capability to predict the occurrence and the temporal evolution of SEP events, it is essential to understand the relative roles of these two major energy-release processes in producing particle acceleration at the Sun. The main difficulty in the analysis of SEP observations is that they are blurred as a result of particle transport through the interplanetary medium. We have relatively good knowledge about SEP transport processes parallel to the magnetic field, but perpendicular transport in the corona and solar wind presents a major problem that is still to be elucidated. Meanwhile, the only way to obtain observational information about solar particle acceleration processes without the effects of interplanetary particle transport is to study the neutral emissions resulting from accelerated particles interacting with the solar atmosphere. Hard X-rays and radio waves give a lot of information on the accelerated electron populations at the Sun as well as on those escaping to the interplanetary medium (e.g., Krucker et al. 2007; Lehtinen et al. 2008; Agueda et al. 2008).

Solar gamma rays (Ramaty and Lingenfelter 1975) and neutrons (Lingenfelter et al. 1965) can be studied to obtain information about interacting ion populations. Measurements of these energetic neutral particles have so far been implemented at 1 AU aboard spacecraft (e.g., Chupp et al. 1982; Kuznetsov et al. 2006) and also by ground-based instrumentation (e.g., Debrunner et al. 1983; Efimov et al. 1983; Chupp et al. 1987). Although new monitoring experiments are being developed (e.g., Matsubara et al. 1999; Tsuchiya et al. 2001), the distance to the Sun severely limits possibilities to study the solar atmospheric energetic ion environment because of sensitivity issues, and also because low-energy neutrons decay before they can reach the observing spacecraft. Sometimes the decay protons and electrons can be identified at 1 AU, thereby providing limited information on the low-energy neutron environment in the solar atmosphere (e.g., Evenson et al. 1983; Kocharov et al. 1996). Planned future solar missions carrying neutron and gamma-ray detectors close to the Sun will be extremely important for future studies of ion acceleration at the Sun (e.g., Kudela et al. 1996; Heber and Klecker 2005; Posner et al. 2005).

An understanding of the roles of different processes contributing to SEP acceleration and release will be essential to allow the provision of reliable forecasts of SEP events. Ultimately, only methods providing reliable detailed forecasts of solar eruptions (the occurrence and properties of flares and CMEs) can take us through to a stage that will act to support reliable SEP forecasting.

Radiation Belt Particles. Work on including wave processes into global radiation belt models is at an early stage and there are many uncertainties concerning the distribution of wave power in MLT, the latitude distribution of the waves and the effectiveness of different types of wave modes. It is essential that databases of all the different wave modes that can contribute to electron acceleration and loss are developed so that the empirical wave models can be improved. Physical models on magnetospheric wave propagation should also be investigated. Kinetic models of the convective transport should be coupled with radiation belt models. There is in addition a need to continue measuring energetic particles as well as the seed population of electrons that power the waves. This in turn must be matched by developments in modeling to incorporate these data, and reproduce more accurately flux variations during magnetic storms and other disturbances, and combining models and observations should have a high priority. This is essential in order to develop reliable space weather prediction capability.

5.2 Outstanding Issues on Engineering Models

Availability, Documentation and Maintenance of the Codes. A plan towards providing a reliable engineering model to forecast radiation belt dynamics in response to changes in the solar wind requires physical, data driven models to become to openly available. The most advanced model in the field (Salammbô), however, is developed through military contracts, and it is not in the public domain. Similarly, ITAR issues prevent users outside the United States from fully benefiting from the latest developments in CR engineering models. These kind of closed source issues severely hinder the development of tools for space weather applications.

Even if the codes were to become available, however, one should in principle still make sure that they are maintained, documented and distributed in a coordinated, efficient and transparent fashion. These issues should be generally solved in order to allow a larger pool of researchers and engineers to participate in the development of space weather prediction tools. There are many examples of open source software projects with contributors world wide, so efficient tools for such distributed code development projects exist. The establishment of a repository of codes maintained by a large scientific and technical collaboration, like COST actions in Europe, could offer a way to tackle present problems.

Validation. Validation by independent users of automatic codes is a key issue in order to estimate their reliability in time. This is true for all kinds of space weather prediction tools. For SEP event occurrence forecasts, the PROTONS code was, for example, validated by (Balch 2008) using SEP data from 1986–2004. It was found by this author that, when the optimal Heidke skill score is used with a probability threshold of 20–30%, the FAR is 57% and the PoD is 55%. The PPS code was validated by Kahler et al. (2007), considering $\geq$ M5 X-ray flares during the interval 1997–2001. Roughly equal numbers of correct and false predictions were associatively found. However, other SEP codes for short-term forecasts have not received independent validation. Thus, it is difficult to judge their relative merits and to select the best code for the purposes of each user.

Many models of the charged-particle radiation environment depend on magnetic field models, and, from the many possible options, it should be possible to choose the best for each particular application. The magnetic field model is, in many cases, decisive for the output of the code (e.g., Desorgher et al. 2009). The selection of the field model is always a compromise between accuracy and efficiency. Therefore, a careful evaluation of the performance (scientific and computational) of the available models should be performed. McCollough et al. (2008) have taken the first important steps in this direction by evaluating the performance of the most commonly used magnetic field models for geostationary orbit. Similar studies should now be performed for other magnetospheric regions.

Availability of Input Data for the Models. Many engineering models of the radiation environment depend on inputs from other models, data and indices. One of the associated problems is to make sure that the essential data and models are available for all the prediction algorithms that can utilize them. Models that depend on publicly available external models and routinely available near-real-time data (with back-up sources) are, in this sense, in the best position. Methods requiring either inputs from non-transparent external models or data with unreliable availability should not be utilized even if they would, in principle, provide satisfactory performance.

Measures to improve the availability of data in standardized formats would of course be very beneficial for modelers developing tools for engineering purposes. One example of such a project is the database of NM data that is currently being constructed in Europe with funding from the EU.

Quality Calibration and Documentation of Source Data. One of the most important issues in tool development is the quality of the input data. Any model relying on external input data has to assume that these data are well calibrated in order to produce reasonable results. Unfortunately, in the case of spacecraft measurements of energetic particle radiation, different instruments often record different fluxes at the same location. Furthermore, typically the methods of how the instrument was calibrated are not released along with the data, so independent evaluation of data quality is almost impossible. It should be common practice to release a description of the calibration procedures employed together with the data, and modelers should demand the provision of this input before using particular data as inputs to their models.

6 Summary and Conclusions

We have reviewed the physical processes affecting, as well as various models describing, the Earth's radiation environment and its dynamics. The present state of the field is in an exciting one since physical understanding of many of the relevant processes has increased to a level, where operational tools relying on physical models have become possible to develop in the future.

The prediction of the GCR environment for space-weather purposes is easiest at the solar-cycle time scale, where simple semi-empirical and engineering models are available to describe the variations relatively accurately. Similar models of short-term changes in response to individual solar eruptions (i.e., Forbush decreases) are still to be developed. SEP models can be divided in event prediction models and statistical fluence/flux models. Advances in the development of both types of models have been achieved recently, but especially in event prediction, we are still far from the ability of reliable forecasting. To achieve this, we need to

identify the most important particle acceleration mechanisms at the Sun, and their relation to observable precursor signals at different wavelengths. Thus, basic research on SEP events is still necessary for enabling advances in space weather prediction capabilities.

Current engineering models for the radiation belts are still empirical models based on combining measured fluxes with models of the Earth's magnetic field, taking account only the phase of the solar cycle and not the momentary activity level of the magnetosphere and its near history. On the other hand, physical models of radiation belt dynamics has evolved to a state, where contributions from individual physical processes to the evolutions of fluxes can be quantitatively assessed. Modeling efforts to utilize data together with physical models have been started and clearly hold a promise of an ability of nowcasting or even forecasting the evolution of the trapped particle fluxes in response to magnetospheric activity.

Several models of the effects of the charged-particle radiation on the ionosphere and atmosphere have also been developed during the recent years. These models enable an accurate computation of the ionization by the precipitating particles, which has important impacts on the atmospheric chemistry and even to the global magnetosphere–ionosphere coupling processes. The use of such models in further research should be advocated.

In conclusion, many of the models describing the dynamics of the Earth's particle radiation environment still require further development and validation using data from present and future spacecraft missions. For this reason, empirical and semi-empirical models will still play an important role in the future modeling of the Earth's particle radiation environment, but the importance of utilizing physics based reanalysis methods will become more and more important in future, especially in developing dynamical models. Measures to improve the engineering models should be implemented by launching new missions to gather further data sets as well as by making more efficient and better use of already existing data.

Acknowledgements This review is based on the activities of the EU COST Action 724, Working Group 2: The Radiation Environment of the Earth, which ran from 2003 to 2007. The authors acknowledge the financial support from the COST action and are grateful to all members of the Working Group for stimulating discussions. We also acknowledge the support from the International Space Sciences Institute in Bern that enabled the authors to work together on the manuscript. RV acknowledges financial support from the Academy of Finland (project 1124837). ML and MS acknowledge financial support from the Italian Space Agency (Bepi-Colombo Mission and ESS2 Project). KK wishes to acknowledge support by VEGA grant agency project No. 2/7063/27. The authors wish to thank the referee for valuable comments on the manuscript.

References

B. Abel, R.M. Thorne, J. Geophys. Res. **103**, 2385 (1998)
J.H. Adams Jr., R. Silberberg, C.H. Tsao, NRL Memo. Rep. **4506** (1981)
N. Agueda, R. Vainio, D. Lario, B. Sanahuja, Astrophys. J. **675**, 1601 (2008)
S.T. Akiniyan, G.A. Bazilevskaya, V.N. Ishkov et al., in *Catalog of Solar Proton Events 1970–1979*, ed. by Yu.I. Logachev. (IZMIRAN, Moscow, 1983), p. 183
K. Alanko-Huotari, I.G. Usoskin, K. Mursula, G.A. Kovaltsov, J. Geophys. Res. **112**, A08101 (2007)
J.M. Albert, J. Geophys. Res. **108** (2003). doi:10.1029/2002JA009792
J.M. Albert, J. Geophys. Res. **110**, A03218 (2005). doi:10.1029/2004JA010844
J.M. Albert, G.P. Ginet, J. Geophys. Res. **103**, 14865 (1998)
J.M. Albert, G.P. Ginet, M.S. Gussenhoven, J. Geophys. Res. **103**, 9261 (1998)
J. Alcaraz et al., Phys. Lett. B **490**, 2 (2000a)
J. Alcaraz et al., Phys. Lett. B **494**, 193 (2000b)
L. Alexandrov, A. Mishev, P. Velinov, C. R. Acad. Bulg. Sci. **61**, 495 (2008)
I.I. Alexeev, Y.I. Feldstein, J. Atmos. Sol.-Terr. Phys. **63**, 431 (2001)
I.I. Alexeev, E.S. Belenkaya, V.V. Kalegaev, Ya.I. Feldstein, A. Grafe, J. Geophys. Res. **101**, 7737 (1996)
J. Allison et al., IEEE Trans. Nucl. Sci. **53**, 270 (2006)
A. Aran, B. Sanahuja, D. Lario, Adv. Space Res. **36**, 2333 (2005a)

A. Aran, B. Sanahuja, D. Lario, Ann. Geophys. **23**, 3047 (2005b)
A. Aran, B. Sanahuja, D. Lario, Adv. Space Res. **37**, 1240 (2006)
D.N. Baker, J.B. Blake, D.J. Gorney, P.R. Higbie, R.W. Klebesadel, J.H. King, Geophys. Res. Lett. **14**, 1027 (1987)
D.N. Baker, S.G. Kanekal, J. Atmos. Sol.-Terr. Phys. **70**, 195 (2008)
C.C. Balch, Rad. Meas. **30**, 231 (1999)
C.C. Balch, Space Weather **6**(1), S01001 (2008)
C.C. Balch, J. Kunches, in *Solar-Terrestrial Predictions*, ed. by P.A. Simon, G. Heckman, M.A. Shea (NOAA, Boulder, 1986), p. 353
F. Ballarini, M. Biaggi, L. De Biaggi, A. Ferrari, A. Ottolenghi et al., Adv. Space Res. **34**, 1338 (2004)
F. Ballarini, D. Alloni, A. Facoetti, A. Mairani, R. Nano, A. Ottolenghi, Adv. Space Res. **40**, 1392 (2007)
D.R. Barraclough, Geophys. J.R. Astron. Soc. **36**, 497 (1974)
J.L. Barth, C.S. Dyer, E.G. Stassinopoulos, IEEE Trans. Nucl. Sci. **50**, 466 (2003)
G.A. Bazilevskaya, E.V. Vashenyuk, V.N. Ishkov et al., Plots of the time profiles and energetic spectra of protons, synoptic charts and schemes of sunspot groups. in *Solar Proton Events. Catalogue 1980–1986*, ed. by Yu.J. Logachev (Soviet Geophysical Committee of the Academy of Science of USSR, Moscow, 1990), p. 160
G.A. Bazilevskaya, I.G. Usoskin, E.O. Flückiger et al., Space Sci. Rev. **137**, 149 (2008)
J. Beer, M. Vonmoos, R. Muscheler, Space Sci. Rev. **125**, 67 (2006)
A. Belov, L. Baisultanova, E. Eroshenko, H. Mavromichalaki, V. Yanke, V. Pchelkin, C. Plainaki, G. Mariatos, J. Geophys. Res. **110** (2005). doi:10.1029/2005JA011067
T. Beutier, D. Boscher, J. Geophys. Res. **100**, 14853 (1995)
J.B. Blake, W.A. Kolasinski, R.W. Fillius, E.G. Mullen, Geophys. Res. Lett. **19**, 821 (1992)
R. Blandford, D. Eichler, Phys. Rep. **154**, 1 (1987)
P.R. Boberg, A.J. Tylka, J.H. Adams, E.O. Flückiger, E.O. Kobel, Geophys. Res. Let. **22**(9), 1133 (1995)
P. Bobik, M. Storini, K. Kudela, E.G. Cordaro, Nuovo Cim. **26**(2), 177 (2003)
P. Bobik, G. Boella, M.J. Boschini, M. Gervasi, D. Grandi, K. Kudela, S. Pensotti, P.G. Rancoita, J. Geophys. Res. **111**, A05205 (2006). doi:10.1029/2005JA011235
D. Boscher, S. Bourdarie, D. Lazaro et al., ONERA Techn. Report RTS 2/06923 DESP (2003)
S. Bourdarie, D. Boscher, T. Beutier, J.A. Sauvaud, M. Blanc, J. Geophys. Res. **102**, 17541 (1997)
D.H. Brautigam, J.M. Albert, J. Geophys. Res. **105**, 291 (2000)
D.H. Brautigam, J.T. Bell, PL-TR-95-2128, Environmental research papers (Phillips Laboratory) (1995), p. 1178
R. Bucik, K. Kudela, I.N. Kuznetsov, Ann. Geophys. **24**, 1969 (2006)
R.A. Burger, M. Hattingh, Astrophys. J. **505**, 244 (1998)
R.A. Burger, M.S. Potgieter, B. Heber, J. Geophys. Res. **105**, 27447 (2000)
R. Bütikofer, E.O. Flückiger, L. Desorgher, *Proc. 30th Internat. Cosmic Ray Conf.*, vol. 1 (2008a), p. 769
R. Bütikofer, E.O. Flückiger, L. Desorgher, M.R. Moser, Sci. Total Envir. **391**, 177 (2008b)
R.A. Caballero-Lopez, H. Moraal, J. Geophys. Res. **109**, A01101 (2004)
J.C. Cain, S.J. Hendricks, R.A. Langel, W.V. Hudson, J. Geomag. Geoelectr. **19**, 335 (1967)
H.V. Cane, R.A. Mewaldt, C.M.S. Cohen, T.T. von Rosenvinge, J. Geophys. Res. **111**, A06S90 (2006). doi:10.1029/2005JA011071
G. Castagnoli, D. Lal, Radiocarbon **22**, 133 (1980)
Y. Chan, G.D. Reeves, R.H.W. Friedel, Nature Phys. **3**, 614 (2007)
D.L. Chenette, J. Chen, E. Clayton, T.G. Guzik, J.P. Wefel, M. Garcia-Muñoz, C. Lopate, K.R. Pyle, K.P. Ray, E.G. Mullen, D.A. Hardy, IEEE Trans. Nucl. Sci. **41**, 2332 (1994)
E.L. Chupp, D.J. Forrest, J.M. Ryan, J. Heslin, C. Reppin, K. Pinkau, G. Kanbach, E. Rieger, G.H. Share, Astrophys. J. **318**, 913 (1982)
E.L. Chupp, H. Debrunner, E.O. Flückiger, D.J. Forrest, F. Golliez, G. Kanbach, W.T. Vestrand, J. Cooper, G. Share, Astrophys. J. **318**, 913 (1987)
J.M. Clem, J.W. Bieber, M. Duldig, P. Evenson, D. Hall, J. Humble, J. Geophys. Res. **102**, 26919 (1997)
E.W. Cliver, H.V. Cane, in *Proc. Solar-Terrestrial Prediction Workshop*, vol. 1, ed. by R.J. Thompson et al., Leura (Australia) (1990), p. 359
E.W. Cliver, D.J. Forrest, H.V. Cane et al., Astrophys. J. **343**, 953 (1989)
D.J. Cooke, J.E. Humble, M.A. Shea et al., Nuovo Cimento C **14**, 213 (1991)
F.A. Cucinotta, *Space Physiology and Medicine*, 5th edn. (2007). http://ntrs.nasa.gov/archive/nasa/casi.ntrs.nasa.gov/20070010704_2007005310.pdf
A. Damiani, M. Storini, M. Laurenza et al., J. Atmos. Sol.-Terr. Phys. **68**, 2042 (2006)
A. Damiani, M. Storini, M. Laurenza et al., Ann. Geophys. **26**, 361 (2008)
H. Debrunner, E.O. Flückiger, E.L. Chupp, D.J. Forrest, in *Proc. 8th Internat. Cosmic Ray Conf.*, vol. 4 (1983), p. 75

M. Demirkol, U. Inan, T. Bell, S. Kanekal, D. Wilkinson, Geophys. Res. Lett. **26**(23), 3557 (1999)
L. Desorgher, E.O. Flückiger, M. Gurtner, M. Moser, R. Bütikofer, Int. J. Modern Phys. A **20**, 6802 (2005)
L. Desorgher, K. Kudela, E.O. Flückiger, R. Bütikofer, M. Storini, V. Kalegaev, Acta Geophys. **57**, 75 (2009). doi:10.2478/s11600-008-0065-3
L.I. Dorman, *Cosmic Rays in the Earth's Atmosphere and Underground* (Kluwer, Dordrecht, 2004), p. 855
L. Dorman, L. Pustil'nik, A. Sternlieb et al., Adv. Space Res. **31**, 847 (2003)
L.I. Dorman, O.A. Danilova, N. Iucci, M. Parisi, N.G. Ptitsyna, M.I. Tyasto, G. Villoresi, Adv. Space Res. **42**, 510 (2008)
Yu.E. Efimov, G.E. Kocharov, K. Kudela, *Proc. 18th Int. Cosmic Ray Conf.*, vol. 10 (1983), p. 276
S.R. Elkington, M.K. Hudson, A.A. Chan, Geophys. Res. Lett. **26**, 3273 (1999)
B. Escudier, S. Rossi, D. Boscher et al., in 53rd Int. Astronautical Congress, Houston (Texas), USA, IAC-02-IAA. 6.3.06, October 10–19 (2002)
P. Evenson, P. Meyer, K.R. Pyle, Astrophys. J. **274**, 875 (1983)
A. Fasso, A. Ferrari, J. Ranft, P.R. Sala, CERN200510, INFNTC_0511, SLACR773 (2005)
W.C. Feldman, E.M.D. Symbalisty, R.A. Roussel-Dupré, J. Geophys. Res. **101**, 5195 (1996)
J. Feynman, T.P. Armstrong, L. Dao-Gibner et al., J. Spacecraft Rockets **27**, 403 (1990)
J. Feynman, G. Spitale, J. Wang et al., J. Geophys. Res. **98**, 13281 (1993)
J. Feynman, A. Ruzmaikin, V. Berdichevsky, J. Atmos. Sol.-Terr. Phys. **64**, 1679 (2002)
L.A. Fisk, W.I. Axford, J. Geophys. Res. **74**, 4973 (1969)
E.O. Flückiger, E. Kobel, J. Geomag. Geoelectr. **42**, 1123 (1990)
E.O. Flückiger, D.F. Smart, M.A. Shea, *Proc. 17th Internat. Cosmic Ray Conf.*, vol. 4 (1981), p. 244
E.O. Flückiger, D.F. Smart, M.A. Shea, J. Geophys. Res. **95**, 1113 (1990)
E.O. Flückiger, R. Bütikofer, L. Desorgher, M.R. Moser, *Proc. 28th Internat. Cosmic Ray Conf.*, vol. 7, (2003), p. 4229
M.-C. Fok, R.B. Horne, N.P. Meredith, S.A. Glauert, J. Geophys. Res. **113**, A03S08 (2008). doi:10.1029/2007JA012558
S.E. Forbush, Phys. Rev. **70**, 771 (1946)
R.H.W. Friedel, G.D. Reeves, T. Obara, J. Atmos. Sol.-Terr. Phys. **64**, 265 (2002)
S.F. Fung, E.V. Bell, L.C. Tan, R.M. Candey, M.J. Golightly, S.L. Huston, J.H. King, R.E. McGuire, Adv. Space Res. **36**(10), 1984 (2005)
S.B. Gabriel, in *COST 724 final report: Developing the Scientific Basis for Monitoring, Modelling and Predicting Space Weather*, ed. by J. Lilensten et al. (COST Office, Brussels, 2008), p. 150
S.B. Gabriel, G.J. Patrick, Space Sci. Rev. **107**(1–2), 55 (2003)
H.A. Garcia, Astrophys. J. **420**, 422 (1994a)
H.A. Garcia, Sol. Phys. **154**, 275 (1994b)
H.A. Garcia, Space Weather **2**, S02002 (2004a). doi:10.1029/2003SW000001
H.A. Garcia, Space Weather **2**, S06003 (2004b). 10.1029/2003SW000035
M. Garcia-Munoz, G.M. Mason, J.A. Simpson, Astrophys. J. **202**, 265 (1975)
A. Genevey, Y. Gallet, C.G. Constable, M. Korte, G. Hulot, Geochem. Geophys. Geosyst. **9**, Q04038 (2008)
L.C. Gentile, J.M. Campbell, E.W. Cliver, H.V. Cane, in: *Proc. Solar-Terrestrial Predictions Workshop*, vol. 2 (Ottawa, 1993), p. 153
J. Giacalone, J. Kóta, Space Sci. Rev. **124**, 277 (2006)
S.A. Glauert, R.B. Horne, J. Geophys. Res. **110**, A04206 (2005). doi:10.1029/2004JA010851
L.J. Gleeson, W.I. Axford, Astrophys. J. **154**, 1011 (1968)
N. Gopalswamy, Geophys. Res. Lett. **30**, 8013 (2003). doi:10.1029/2003GL017277
J.C. Green, M.G. Kivelson, J. Geophys. Res. **109**, A03213 (2004). doi:10.1029/2003JA010153
P.K.F. Grieder, *Cosmic Rays at Earth* (Elsevier, Amsterdam, 2001), p. 1093
B. Heber, B. Klecker, Adv. Space Res. **36**(8), 1387 (2005)
D. Heck, Forschungszentrum Karlsruhe Report FZKA 7254 (2006)
G.R. Heckman, in *Solar-Terrestrial Predictions*, vol. 1, ed. by R.F. Donnelley (US Dept. of Commerce, Washington, 1979), p. 322
G.R. Heckman, J.M. Kunches, J.H. Allen, Adv. Space Res. **12**(2–3), 313 (1992)
D. Heynderickx, M. Kruglanski, V. Pierrard, J. Lemaire, M.D. Looper, J.B. Blake, IEEE Trans. Nucl. Sci. **46**, 1475 (1999)
A. Hilgers, A. Glover, E. Daly, in *Space Weather Physics and Effects*, ed. by V. Bothmer, I.A. Daglis. (Springer/Praxis, Berlin, 2007), p. 353
J.L. Hoff, L.W. Townsend, IEEE Trans. Nucl. Sci. **50**(6), 2296 (2003)
A. Holmes Siedle, L. Adams, *Handbook of Radiation Effects*, 2nd edn. (Oxford University Press, Oxford, 2002)
R.B. Horne, in *Review of Radio Science 1999–2002*, ed. by W.R. Stone (Wiley, Bognor Regis, 2002), p. 801
R.B. Horne, Nature Phys. **3**, 590 (2007)

R.B. Horne, R.M. Thorne, Geophys. Res. Lett. **25**, 3011 (1998)
R.B. Horne, N.P. Meredith, R.M. Thorne, D. Heynderickx, R.H.A. Iles, R.R. Anderson, J. Geophys. Res. **108**(A1) 1016 (2003a). doi:10.1029/2002JA0099165
R.B. Horne, S.A. Glauert, R.M. Thorne, Geophys. Res. Lett. **30**(9), 1493 (2003b). doi:10.1029/2003GL016963
R.B. Horne, R.M. Thorne, Y.Y. Shprits, N.P. Meredith, S.A. Glauert, A.J. Smith, S.G. Kanekal, D.N. Baker, M.J. Engebretson, J.L. Posch, M. Spasojevic, U.S. Inan, J.S. Pickett, P.M.E. Decreau, Nature **437**, 227 (2005a)
R.B. Horne, R.M. Thorne, S.A. Glauert, J.M. Albert, N.P. Meredith, R.R. Anderson, J. Geophys. Res. **110**, A03225 (2005b). doi:10.1029/2004JA010811
R.B. Horne, N.P. Meredith, S.A. Glauert, A. Varotsou, D. Boscher, R.M. Thorne, Y.Y. Shprits, R.R. Anderson, in *Recurrent Magnetic Storms: Corotating Solar Wind Streams*, ed. by B.T. Tsurutani, R.L. McPherron, W.D. Gonzalez, G. Lu, J.H.A. Sobral, N. Gopalswamy, Geophys. Monogr. Series, vol. 167 (AGU, Washington, 2006), p. 151
R.B. Horne, R.M. Thorne, S.A. Glauert, N.P. Meredith, D. Pokhotelov, O. Santolik, Geophys. Res. Lett. **34**, L17107 (2007). doi:10.1029/2007GL030267
M.K. Hudson, A.D. Kotelnikov, X. Li, I. Roth, M. Temerin, J. Wygant, J.B. Blake, M.S. Gussenhoven, Geophys. Res. Lett. **22**, 291 (1995)
S.L. Huston, NASA/CR-2002-211784 (2002)
S.L. Huston, K.A. Pfitzer, NASA/CR-1998-208593 (1998)
ICRP, *International Commission on Radiobiological Protection, ICRP Report 60* (Pergamon, Oxford, 1990)
ICRP, *International Commission on Radiobiological Protection, ICRP Report 73* (Pergamon, Oxford, 1993)
R.H.A. Iles, N.P. Meredith, A.N. Fazakerley, R.B. Horne, J. Geophys. Res. **111**, A03204 (2006). doi:10.1029/2005JA011206
C.H. Jackman, R.D. McPeters, in *Solar Variability and its Effects on Climate*, ed. by J.M. Pap, P. Fox, C. Frohlich, H.S. Hudson, J. Kuhn, J. McCormack, G. North, W. Sprigg, S.T. Wu, Geophys. Monogr. Series, vol. 141 (AGU, Washington, 2004), p. 305
C.H. Jackman, D.R. Marsh, F.M. Vitt et al., Atmos. Chem. Phys. **8**, 765 (2008)
D.C. Jensen, J.C. Cain, J. Geophys. Res. **67**, 3568 (1962)
J.R. Jokipii, Astrophys. J. **146**, 480 (1966)
J.R. Jokipii, D.A. Kopriva, Astrophys. J. **234**, 384 (1979)
I. Jun, R.T. Swimm, A. Ruzmaikin et al., Adv. Space Res. **40**, 304 (2007a)
I. Jun, R.T. Swimm, J. Feynman et al., in *Roundtable Meeting on Solar Energetic Particle Environment Modelling*, Southampton, UK (2007b)
S.W. Kahler, J. Geophys. Res. **87**, 3439 (1982)
S.W. Kahler, E.W. Cliver, A.G. Ling, J. Atmos. Sol.-Terr. Phys. **69**, 43 (2007)
Y. Katoh, Y. Omura, Geophys. Res. Lett. **34**, L03102 (2007). doi:10.1029/2006GL028594
T. Kawata, H. Ito, K. George, H. Wu, F.A. Gucinotta, Biol. Sci. Space **18**, 216 (2004)
J.H. King, J. Spacecraft Rockets **11**(6) 401 (1974)
A.L. Kiplinger, Astrophys. J. **453**, 973 (1995)
Z. Klos, H. Rothkaehl, Z. Zbyszyski, S. Kuznetsov, O. Gregorian, N.I. Budko, I.S. Prutensky, S.A. Pulinets, in *Plasma 97: Research and Applications of Plasmas*, ed. by M. Sadowski, H. Rothkaehl (1997), p. 1
D.M. Koch, D.J. Jacob, W.C. Graustein, J. Geophys. Res. **101**(D13), 18651 (1996)
L.G. Kocharov, J. Torsti, R. Vainio, G.A. Kovaltsov, I.G. Usoskin, Sol. Phys. **169**, 181 (1996)
L. Kocharov, R. Vainio, G.A. Kovaltsov, J. Torsti, Sol. Phys. **182**, 195 (1998)
J. Koller, Y. Chen, G.D. Reeves, R.H.W. Friedel, T.E. Cayton, J.A. Vrugt, J. Geophys. Res. **112**, A06244 (2007). doi:10.1029/2006JA012196
D. Kondrashov, Y. Shprits, M. Ghil, R. Thorne, J. Geophys. Res. **112**, A10227 (2007). doi:10.1029/2007JA012583
M. Korte, C.G. Constable, Geochem. Geophys. Geosystems **6**, Q02H16 (2005)
J. Kota, J.R. Jokipii, Astrophys. J. **265**, 573 (1983)
J. Kota, Nucl. Phys. B Proc. Suppl. **39A**, 111 (1995)
B.T. Kress, M.K. Hudson, P.L. Slocum, Geophys. Res. Lett. **32**, 6 (2005)
A.A. Krivolutsky, Adv. Space Res. **31**, 2127 (2003)
S. Krucker, E.P. Kontar, S. Christe, R.P. Lin, Astrophys. J. **663**, L109 (2007)
Y. Kubo, M. Akioka, Space Weather **2**, S01002 (2004). doi:10.1029/2003SW000022
K. Kudela, I. Usoskin, Czechoslovak J. Phys. **54**(2), 239 (2004)
K. Kudela, S.N. Kuznetsov, A. Antalova, Adv. Space Res. **17**(3), 49 (1996)
K. Kudela, M. Storini, M.Y. Hofer, A. Belov, Space Sci. Rev. **93**, 153 (2000)
K. Kudela, R. Bucik, P. Bobik, Adv. Space Res. **42**(7), 1300 (2008)
V. Kurt, A. Belov, H. Mavromichalaki, M. Gerontidou, Ann. Geophys. **22**(6), 2255 (2004)

T. Kuwabara, J.W. Bieber, J. Clem et al., Space Weather **4**, S10001 (2006). doi:10.1029/2006SW000223
N.V. Kuznetsov, R.A. Nymmik, M.I. Panasyuk, Adv. Space Res. **36**, 2003 (2005)
S.N. Kuznetsov, V.G. Kurt, I.N. Myagkova, B.Yu. Yushkov, K. Kudela, Sol. System Res. **40**(2), 104 (2006)
S.T. Lai, A Critical Overview on Spacecraft Charging Mitigation Methods (Air Force Res. Lab. Hanscom AFB, MA, Space Weather Center of Excellence) (2003). http://handle.dtic.mil/100.2/ADA423290
C. Laj, C. Kissel, A. Mazaud, J.E.T. Channell, J. Beer, Phil. Trans. R. Soc. Lond. **358**, 1009 (2000)
C. Laj, C. Kissel, A. Mazaud, E. Michel, R. Muscheler, J. Beer, Earth Planet. Sci. Lett. **200**, 177 (2002)
M.M. Lam, R.B. Horne, N.P. Meredith, S.A. Glauert, Geophys. Res. Lett. **34**, L20112 (2007). doi:10.1029/2007GL030267
U.W. Langner, M.S. Potgieter, H. Fichtner, T. Borrmann, Astrophys. J. **640**, 1119 (2006)
D. Lario, B. Sanahuja, A.M. Heras, Astrophys. J. **509**, 415 (1998)
J.-M. Lauenstein, J.L. Barth, IEEE Radiation Effects Data Workshop, p. 102, 2005. doi:10.1109/REDW.2005.1532674
M. Laurenza, J. Hewitt, E.W. Cliver et al., Contribution to 20th ECRS, September 5–8, 2006, Lisbon, Portugal (2007). Available at http://www.lip.pt/events/2006/ecrs/proc/ecrs06-s1-34.pdf
M. Laurenza, E.W. Cliver, J. Hewitt, M. Storini, A.G. Ling, C.C. Balch, M.L. Kaiser, Space Weather, 2007SW000379 (2009, in press)
J.A. le Roux, G.M. Webb, V. Florinski, G.P. Zank, Astrophys. J. **662**, 350 (2007)
M.A. Lee, Astrophys. J. Suppl. **158**, 38 (2005)
N. Lehtinen, S. Pohjolainen, K. Huttunen-Heikinmaa, R. Vainio, E. Valtonen, A.E. Hillaris, Sol. Phys. **247**, 151 (2008)
F. Lei, A. Hands, S. Clucas, C. Dyer, P. Truscott, IEEE Trans. Nucl. Sci. **53**, 1851 (2006)
X. Li, M.A. Temerin, Space Sci. Rev. **95**, 569 (2001)
X. Li, D.N. Baker, M. Temerin, D. Larson, R.P. Lin, G.D. Reeves, M. Looper, S.G. Kanekal, R.A. Mewaldt, Geophys. Res. Lett. **24**, 923 (1997)
N. Lifton, D.F. Smart, M.A. Shea, Earth Planet. Sci. Lett. **268**, 190 (2008)
R.E. Lingenfelter, E.J. Flamm, E.H. Canfield, S. Kellman, J. Geophys. Res. **70**, 4087 (1965)
Yu.E. Litvinenko, Sol. Phys. **212**, 379 (2003)
S. Liu, V. Petrosian, G.M. Mason, Astrophys. J. **613**, L81 (2004)
M. Lockwood, R. Stamper, M.N. Wild, Nature **399**, 437 (1999)
M.D. Looper, J.B. Blake, R.A. Mewaldt, Geophys. Res. Lett. **32**, L03 S06 (2005). doi:10.1029/2004GL021502
K.R. Lorentzen, M.P. McCarthy, G.K. Parks, J.E. Foat, R.M. Millan, D.M. Smith, R.P. Lin, J.P. Treilhou, J. Geophys. Res. **105**, 5381 (2000)
K.R. Lorentzen, J.E. Mazur, M.D. Looper, J.F. Fennell, J.B. Blake, J. Geophys. Res. **107**, 1231 (2002). doi:10.1029/2001JA000276
L.R. Lyons, R.M. Thorne, J. Geophys. Res. **78**, 2142 (1973)
G. Mann, H. Aurass, A. Warmuth, Astron. Astrophys. **454**, 969 (2006)
J. Masarik, J. Beer, J. Geophys. Res. **104**(D10), 12099 (1999)
R.A. Mathie, I.R. Mann, Geophys. Res. Lett. **27**, 3261 (2000)
Y. Matsubara, Y. Muraki, K. Masuda et al., *Proc. 26th Internat. Cosmic Ray Conf.*, vol. 6 (1999), p. 42
H. Mavromichalaki, C. Plainaki, M. Gerontidou et al., IEEE Trans. Nucl. Sci. **54**(4), 1082 (2007)
J.P. McCollough, J.L. Gannon, D.N. Baker, M. Gehmeyr, Space Weather **6**, S10001 (2008). doi:10.1029/2008SW000391
K.G. McCracken, F. McDonald, J. Beer, G. Raisbeck, F. Yiou, J. Geophys. Res. **109**, A12103 (2004)
K. McCracken, J. Beer, J. Geophys. Res. **112**, A10101 (2007)
F.B. McDonald (ed.), *Solar Proton Manual, NASA TR R-169* (NASA, Washington, 1963)
M.W. McElhinny, W.E. Senanayake, J. Geomagn. Geoelectr. **34**, 39 (1982)
C.E. McIlwain, J. Geophys. Res. **66**, 3681 (1961)
S. McKenna-Lawlor, in *COST 724 Final Report: Developing the Scientific Basis for Monitoring, Modelling and Predicting Space Weather*, ed. by J. Lilensten et al. (COST Office, Brussels, 2008), p. 179
J.D. Meffert, M.S. Gussenhoven, PL-TR-94-2218, Environmental Research Papers, 1158, Phillips Laboratory (1994)
N.P. Meredith, A.D. Johnstone R, B. Horne, R.R. Anderson, J. Geophys. Res. **105** (2000)
N.P. Meredith, R.B. Horne, R.R. Anderson, J. Geophys. Res. **106**, 13165 (2001)
N.P. Meredith, M. Cain, R.B. Horne, R.M. Thorne, D. Summers, R.R. Anderson, J. Geophys. Res. **108**(A6), 1248 (2003a). doi:10.1029/2002JA009764
N.P. Meredith, R.M. Thorne, R.B. Horne, D. Summers, B.J. Fraser, R.R. Anderson, J. Geophys. Res. **108**, 1250 (2003b). doi:10.1029/2002JA009700
N.P. Meredith, R.B. Horne, R.M. Thorne, R.R. Anderson, Geophys. Res. Lett. **30**, 1871 (2003c). doi:10.1029/2003GL017698

N.P. Meredith, R.B. Horne, S.A. Glauert, R.M. Thorne, D. Summers, J.M. Albert, R.R. Anderson, J. Geophys. Res. **101**, A05212 (2006). doi:10.1029/2005JA011516
R.M. Millan, R.P. Lin, D.M. Smith, K.R. Lorentzen, M.P. McCarthy, Geophys. Res. Lett. **29**(24), 2194 (2002). doi:10.1029/2002GL015922
R.M. Millan, R.P. Lin, D.M. Smith, M.P. McCarthy, Geophys. Res. Lett. **34**, L10101 (2007). doi:10.1029/2006GL028653
Y. Miyoshi, A. Morioka, H. Misawa, Geophys. Res. Lett. **27**, 2169 (2000)
Y.S. Miyoshi, V.K. Jordanova, A. Morioka, M.F. Thomsen, G.D. Reeves, D.S. Evans, J.C. Green, J. Geophys. Res. **111**, A11S02 (2006). doi:10.1029/2005JA011351
J.L. Modisette, T.M. Vinson, A.C. Hardy, NASA TN D-2746, (Washington, D.C., 1965)
I.V. Moskalenko, A.W. Strong, J.F. Ormes, M.S. Potgieter, Astrophys. J. **565**, 280 (2002)
R. Muscheler, J. Beer, P.W. Kubik, H.A. Synal, Quaternary Sci. Rev. **24**(16–17), 1849 (2005)
H.V. Neher, J. Geophys. Res. **72**, 1527 (1967)
H.V. Neher, J. Geophys. Res. **76**, 1637 (1971)
C.K. Ng, D.V. Reames, Astrophys. J. **424**, 1032 (1994)
C.K. Ng, D.V. Reames, Astrophys. J. Lett. **686**, L123 (2008)
B. Ni, R.M. Thorne, Y.Y. Shprits, J. Bortnik, Geophys. Res. Lett. **35**, L11106 (2008). doi:10.1029/2008GL034032
J.H. Nonnast, T.P. Armstrong, J.W. Kohl, J. Geophys. Res. **87**, 4327 (1982)
R.A. Nymmik, *Proc. 25th Internat. Cosmic Ray Conf.*, vol. 6 (1999a), p. 268
R.A. Nymmik, *Proc. 25th Internat. Cosmic Ray Conf.*, vol. 6 (1999b), p. 280
R.A. Nymmik, Rad. Meas. **30**, 287 (1999c)
R.A. Nymmik, *Proc. 27th Internat. Cosmic Ray Conf.* (2001), p. 3197
R.A. Nymmik, in *COST 724 Final Report: Developing the Scientific Basis for Monitoring, Modelling and Predicting Space Weather*, ed. by J. Lilensten et al. (COST Office, Brussels, 2008), p. 159
R.A. Nymmik, M.I. Panasyuk, A.A. Suslov, Adv. Space Res. **17**, 19 (1996)
R.A. Nymmik, M.I. Panasyuk, V.V. Petrukhin, B.Y. Yushkov, *Proc. 30th Internat. Cosmic Ray Conf.*, vol. 1 (2008), p. 701
K. O'Brien, in *Proc. 7th Internat. Symp. on the Natural Radiation Environment*, ed. by J.P. McLaughlin, S.E. Simopoulos, F. Steinhusler (Elsevier, Amsterdam, 2005), p. 29
P. O'Brien, Private Communication (2008)
W.P. Olson, K.A. Pfitzer, J. Geophys. Res. **79**, 3739 (1974)
P.M. O'Neill (2007). http://ntrs.nasa.gov/archive/nasa/casi.ntrs.nasa.gov/20070009876_2007007169.pdf
Y.J. Orsolini, G.L. Manney, M.L. Santee, C.E. Randall, Geophys. Res. Lett. **32**, L12S01 (2005). doi:10.1029/2004GL021588
E. Pallé, C.J. Butler, K. O'Brien, J. Atmos. Sol.-Terr. Phys. **66**, 1779 (2004)
E.N. Parker, Planet. Space Sci. **13**(1), 9 (1965)
M. Pelliccioni, Radiat. Prot. Dosim. **88**, 279 (2000)
D. Pokhotelov, W. Lotko, A.V. Streltsov, Ann. Geophys. **22**, 2943 (2004)
A. Posner, Space Weather **5**, S05001 (2007). doi:10.1029/2006SW000268
A. Posner, D.M. Hassler, D.J. McComas, S. Rafkin, R.F. Wimmer-Schweingruber, E. Bohm, S. Bottcher, S. Burmeister, W. Dröge, B. Heber, Adv. Space Res. **36**(8), 1426 (2005)
S.A. Pulinets, EOS **88**(20), 217 (2007)
G.M. Raisbeck, F. Yiou, M. Fruneau et al., Geophys. Res. Lett. **8**, 1015 (1981)
R. Ramaty, R.E. Lingenfelter, in: Solar gamma-, X-, and EUV radiation; Proceedings of the Symposium, Buenos Aires, Argentina, June 11–14, 1974, (D. Reidel, Dordrecht, 1975), p. 363
C.E. Randall, V.L. Harvey, G.L. Manney et al., Geophys. Res. Lett. **32**, L05802 (2005). doi:10.1029/2004GL022003
D.V. Reames, Space Sci. Rev. **90**, 413 (1999)
W.K.M. Rice, G.P. Zank, G. Li, J. Geophys. Res. **108**, 1369 (2003). doi:10.1029/2002JA009756
D.J. Rodgers, K.A. Hunter, G.L. Wrenn, Proc. 8th Spacecraft Charging Technology Conference, Huntsville, Alabama, NASA/CP-2004-213091 (2004)
E.C. Roelof, in: H. Ögelman, J.R. Wayland, Lectures in High-Energy Astrophysics, NASA SP-199 (1969), p. 111
H. Rothkaehl, Z. Klos, Adv. Space Res. **31**, 5 (2003)
H. Rothkaehl, M. Parrot, J. Atm. Sol.-Terr. Phys. **67**, 821 (2005)
H. Rothkaehl, R. Bucik, K. Kudela, Phys. Chem. Earth **31**, 473 (2006)
D. Ruffolo, Astrophys. J. **382**, 688 (1991)
D. Ruffolo, Astrophys. J. **442**, 861 (1995)
B. Sanahuja, A. Aran, D. Lario, in *COST 724 Final Report: Developing the Scientific Basis for Monitoring, Modelling and Predicting Space Weather*, ed. by J. Lilensten et al. (COST Office, Brussels, 2008), p. 215

A. Sandroos, R. Vainio, Astrophys. J. **662**, L127 (2007)
D.M. Sawyer, J.I. Vette, NSSDC/WDC-A-R&S 76-06 (1976)
K. Scherer, H. Fichtner, T. Borrmann et al., Space Sci. Rev. **127**, 327 (2006)
R.S. Selesnick, M.D. Looper, R.A. Mewaldt, Space Weather **5**, S04003 (2007). doi:10.1029/2006SW000275
M.A. Shea, D.F. Smart, Sol. Phys. **127**, 297 (1990)
M.A. Shea, D.F. Smart, Adv. Space Res. **34**, 420 (2004)
M.A. Shea, D.F. Smart, L.C. Gentile, Phys. Earth Plan. Int. **48**, 200 (1987)
Y.Y. Shprits, R.M. Thorne, Geophys. Res. Lett. **31**, L08805 (2004). doi:10.1029/2004GL019591
Y.Y. Shprits, W. Li, R.M. Thorne, J. Geophys. Res. **111**, A12206 (2006a). doi:10.1029/2006JA011758
Y.Y. Shprits, R.M. Thorne, R.B. Horne, S.A. Glauert, M. Cartwright, C.T. Russell, D.N. Baker, S.G. Kanekal, Geophys. Res. Lett. **33**, L05104 (2006b). doi:10.1029/2005GL024256
Y. Shprits, D. Kondrashov, Y. Chen, R. Thorne, M. Ghil, R. Friedel, G. Reeves, J. Geophys. Res. **112**, A12216 (2007). doi:10.1029/2007JA012579
Y.Y. Shprits, S.R. Elkington, N.P. Meredith et al., J. Atmos. Sol.-Terr. Phys. **70**, 1679 (2008a)
Y.Y. Shprits, D.A. Subbotin, N.P. Meredith et al., J. Atmos. Sol.-Terr. Phys. **70**, 1694 (2008b)
A. Sicard-Piet, S. Bourdarie, D. Boscher, R.H.W. Friedel, IEEE Trans. Nucl. Sci. **53**, 1844 (2006)
A.S. Sicard-Piet, D. Bourdarie, R.H. Boscher, W. Friedel, M. Thomsen, T. Goka, H. Matsumoto, H. Koshiishi, Space Weather **6**, S07003 (2008). doi:10.1029/2007SW000368
S.F. Singer, Phys. Rev. Lett. **1**, 171 (1958)
A.I. Sladkova, G.A. Bazilevskaya, V.N. Ishkov et al., in *Catalogue of Solar Proton Events 1987–1996*, ed. by Y. Logachev (University Press, Moscow, 1998)
D.F. Smart, M.A. Shea, in *Solar-Terrestrial Predictions*, vol. 1, ed. by R.F. Donnelley (US Dept. of Commerce, Washington, 1979), p. 406
D.F. Smart, M.A. Shea, Adv. Space Res. **9**(10), 281 (1989)
D.F. Smart, M.A. Shea, *Proc. 30th Internat. Cosmic Ray Conf.*, vol. 1 (2008a), p. 733
D.F. Smart, M.A. Shea, *Proc. 30th Internat. Cosmic Ray Conf.*, vol. 1 (2008b), p. 737
D.F. Smart, M.A. Shea, E.O. Flückiger, A.J. Tylka, P.R. Boberg, *Proc. 26th Int. Cosmic Ray Conf.*, vol. 7 (1999), p. 398
D.F. Smart, M.A. Shea, E.O. Flückiger, Space Sci. Rev. **93**, 305 (2000)
D.F. Smart, M.A. Shea, A.J. Tylka, P.R. Boberg, Adv. Space Res. **37**(6), 1206 (2006)
S.K. Solanki, M. Schüssler, M. Fligge, Nature **408**, 445 (2000)
S.K. Solanki, I.G. Usoskin, B. Kromer, M. Schüssler, J. Beer, Nature **431**, 1084 (2004)
E.G. Stassinopoulos, NSSDC 75-11, (NASA, Greenbelt, 1975)
M. Storini, A. Damiani, *Proc 30th Internat. Cosmic Ray Conf.*, vol. 1 (2008), p. 277
M. Storini, G.A. Bazilevskaya, E.O. Flueckiger et al., Adv. Space Res. **31**(4), 895 (2003)
M. Storini, P. Diego, C. Grimani et al., in *Contributions to EGU2008, Report INAF/IFSI-2008-8*, ed. by A. Gardini. (INAF/IFSI, Roma, 2008a), p. 3
M. Storini, P. Metteo, G. Moreno, Adv. Space Res. **41**, 70 (2008b)
M. Storini, E.W. Cliver, M. Laurenza et al., in *COST 724 Final Report: Developing the Scientific Basis for Monitoring, Modelling and Predicting Space Weather*, ed. by J. Lilensten et al. (COST Office, Brussels, 2008c), p. 63
D. Summers, C. Ma, J. Geophys. Res. **105**, 15887 (2000)
D. Summers, R.M. Thorne, J. Geophys. Res. **108**, 1143 (2003). doi:10.1029/2002JA009489
D. Summers, R.M. Thorne, F. Xiao, J. Geophys. Res. **103**, 20487 (1998)
D. Summers, C. Ma, N.P. Meredith, R.B. Horne, R.M. Thorne, R.R. Anderson, J. Atmos. Sol.-Terr. Phys. **66**, 133 (2004)
Z. Svestka, P. Simon (eds.), *Catalog of Solar Particle Events 1955–1969, Astrophysics and Space Science Library* (Reidel, Dordrecht, 1975)
R.M. Thorne, Science **197**, 287 (1977)
I.N. Toptygin, *Cosmic Rays in Interplanetary Magnetic Fields* (Kluwer, Dordrecht, 1985)
V.Y. Trakhtengerts, M.J. Rycroft, D. Nunn, A.G. Demekhov, J. Geophys. Res. **108**, 1138 (2003)
H. Tsuchiya, Y. Muraki, K. Masuda et al., Nucl. Instrum. Meth. A **463**, 183 (2001)
N.A. Tsyganenko, Planet. Space Sci. **37**, 5 (1989)
N.A. Tsyganenko, J. Geophys. Res. **100**, 5599 (1995)
N.A. Tsyganenko, *Proc. 3rd Internat., Conf. on Substorms*, Versailles, France. ESA SP-389 (1996), p. 181
N.A. Tsyganenko, M.I. Sitnov, J. Geophys. Res. **110**, A03208 (2005)
M.I. Tyasto, O.A. Danilova, L.I. Dorman, V.M. Dvornikov, V.E. Sdobnov, Adv. Space Res. **42**(9), 1556 (2008). doi:10.1016/j.asr.2007.06.057
A.J. Tylka, J.H. Adams Jr., P.R. Boberg et al., IEEE Trans. Nucl. Sci. **44**, 2150 (1997)
A.J. Tylka, C.M.S. Cohen, W.F. Dietrich et al., Astrophys. J. **625**, 474 (2005)
I.G. Usoskin, G.A. Kovaltsov, J. Geophys. Res. **111**, D21206 (2006)

I.G. Usoskin, G.A. Kovaltsov, C. R. Geosci. **340**(7), 441 (2008a)
I.G. Usoskin, G.A. Kovaltsov, J. Geophys. Res. **113**(D12), D12107 (2008b). doi:10.1029/2007JD009725
I.G. Usoskin, K. Alanko, K. Mursula, G.A. Kovaltsov, Sol. Phys. **207**, 389 (2002a)
I.G. Usoskin, K. Mursula, S.K. Solanki, M. Schuessler, G.A. Kovaltsov, J. Geophys. Res. **107**(A11), 1374 (2002b)
I.G. Usoskin, O.G. Gladysheva, G.A. Kovaltsov, J. Atmos Sol.-Terr. Phys. **66**, 1791 (2004)
I.G. Usoskin, K. Alanko-Huotari, G.A. Kovaltsov, K. Mursula, J. Geophys. Res. **110**, A12108 (2005)
I.G. Usoskin, S.K. Solanki, C. Taricco, N. Bhandari, G.A. Kovaltsov, Astron. Astrophys. **457**, L25 (2006)
I.G. Usoskin, S.K. Solanki, G.A. Kovaltsov, Astron. Astrophys. **471**, 301 (2007)
I.G. Usoskin, M. Korte, G.A. Kovaltsov, Geophys. Res. Lett. **35**, L05811 (2008)
I.G. Usoskin, L. Desorgher, P. Velinov et al., Acta Geophys. **57**, 88 (2009a)
I.G. Usoskin, C.V. Field, G.A. Schmidt, A. Leppänen, A. Aldahan, G.A. Kovaltsov, G. Possnert, R.K. Ungar, J. Geophys. Res. **114** (2009b). doi:10.1029/2008JD011333
A. Vacaresse, D. Boscher, S. Bourdarie, M. Blanc, J.A. Sauvaud, J. Geophys. Res. **104**, 28601 (1999)
R. Vainio, Astron. Astrophys. **406**, 735 (2003)
R. Vainio, T. Laitinen, Astrophys. J. **658**, 622 (2007)
R. Vainio, T. Laitinen, J. Atmos. Sol.-Terr. Phys. **70**, 467 (2008)
R. Vainio, L. Kocharov, T. Laitinen, Astrophys. J. **528**, 1015 (2000)
A.L. Vampola, Final Report of ESA/ESTEC Contract No. ESA/ESTEC/WMA/P.O.151351 (1996)
M.A.I. Van Hollebeke, J.R. Wang, F.B. McDonald, Catalogue of solar cosmic ray events, IMPs IV and V (May 1967–December 1972), NASA/GSFC X-661-74-27 (1974)
M.A.I. Van Hollebeke, L.S. Ma Sung, F.B. McDonald, Sol. Phys. **41**, 189 (1975)
A. Varotsou, D. Boscher, S. Bourdarie, R.B. Horne, S.A. Glauert, N.P. Meredith, Geophys. Res. Lett. **32**, L19106 (2005). doi:10.1029/2005GL023282
A. Varotsou, D. Boscher, S. Bourdarie, R.B. Horne, N.P. Meredith, S.A. Glauert, R.H. Friedel, J. Geophys. Res. **113**, A12212 (2008). doi:10.1029/2007JA012862
G.I. Vasilyev, V.M. Ostryakov, A.K. Pavlov, J. Atmos. Sol.-Terr. Phys. **70**(16), 2000 (2008)
P. Velinov, L. Mateev, J. Atmos. Sol.-Terr. Phys. **70**, 574 (2008)
P. Velinov, A. Mishev C. R. Acad. Bulg. Sci. **60**(5), 493 (2007)
P.T. Verronen, A. Seppälä, E. Kyrölä et al., Geophys. Res. Lett. **33**, L24811 (2006). doi:10.1029/2006GL028115
J.I. Vette, NSSDC/WDC-A-R&S 91-24 (1991)
M. Vonmoos, J. Beer, R. Muscheler, J. Geophys. Res. **111**, A10105 (2006)
G. Wagner, J. Masarik, J. Beer, S. Baumgartner, D. Imboden, P.W. Kubik, H.-A. Synal, M. Suter, Nucl. Instr. Meth. Phys. Res. **172**, 597 (2000)
Waterman et al., Space Sci. Rev. (2009, this issue)
W.R. Webber, P.R. Higbie, J. Geophys. Res. **108**(A9), 1355 (2003)
W.R. Webber, R.L. Golden, S.J. Stochaj, J.F. Ormes, R.E. Strittmatter, Astrophys. J. **380**, 230 (1991)
W.R. Webber, P.R. Higbie, K.G. McCracken, J. Geophys. Res. **112**, A10106 (2007)
R.S. White, Rev. Geophys. **11**, 595 (1973)
M.A. Xapsos, J.L. Barth, E.G. Stassinopoulos et al., NASA/TP-1999-209763 (Marshall Space Flight Center, Alabama, 1999a)
M.A. Xapsos, G.P. Summers, J.L. Barth et al., IEEE Trans. Nucl. Sci. **46**, 1481 (1999b)
M.A. Xapsos, G.P. Summers, J.L. Barth et al., IEEE Trans. Nucl. Sci. **47**, 486 (2000)
M.A. Xapsos, C. Stauffer, G.B. Gee et al., IEEE Trans. Nucl. Sci. **51**, 3394 (2004)
M.A. Xapsos, C. Stauffer, T. Jordan et al., IEEE Trans. Nucl. Sci. **54**, 1985 (2007)
S. Yang, H. Odah, J. Shaw, Geophys. J. Int. **140**, 158 (2000)
G.P. Zank, G. Li, O.P. Verkhoglyadova, Space Sci. Rev. **130**, 255 (2007)